Impact of dust addition on Mediterranean plankton communities under present and future conditions of pH and temperature: an experimental overview

Frédéric Gazeau[1], Céline Ridame[2], France Van Wambeke[3], Samir Alliouane[1], Christian Stolpe[1], Jean-Olivier Irisson[1], Sophie Marro[1], Jean-Michel Grisoni[4], Guillaume De Liège[4], Sandra Nunige[3], Kahina Djaoudi[3], Elvira Pulido-Villena[3], Julie Dinasquet[5,6], Ingrid Obernosterer[6], Philippe Catala[6], Cécile Guieu[1]

[1] Sorbonne Université, CNRS, Laboratoire d'Océanographie de Villefranche, LOV, 06230 Villefranche-sur-Mer, France

[2] CNRS-INSU/IRD/MNHN/UPMC, LOCEAN: Laboratoire d'Océanographie et du Climat: Expérimentation et Approches Numériques, UMR 7159, 75252 Paris Cedex 05, France

[3] Aix-Marseille Université, Université de Toulon, CNRS/INSU, IRD, MIO, UM 110, 13288, Marseille, France

[4] Sorbonne Université, CNRS, Institut de la Mer de Villefranche, IMEV, 06230 Villefranche-sur-Mer, France

[5] Scripps Institution of Oceanography, University of California San Diego, USA

[6] CNRS, Sorbonne Université, Laboratoire d'Océanographie Microbienne, LOMIC, F-66650 Banyuls-sur-Mer, France

Correspondence to: Frédéric Gazeau (f.gazeau@obs-vlfr.fr)

Keywords: Mediterranean Sea; Atmospheric deposition; Plankton community; Ocean acidification; Ocean warming

Abstract

In Low Nutrient Low Chlorophyll areas, such as the Mediterranean Sea, atmospheric fluxes represent a considerable external source of nutrients likely supporting primary production especially during periods of stratification. These areas are expected to expand in the future due to lower nutrient supply from sub-surface waters caused by climate-driven enhanced stratification, likely further increasing the role of atmospheric deposition as a source of new nutrients to surface waters. Whether plankton communities will react differently to dust deposition in a warmer and acidified environment remains, however, an open question. The potential impact of dust deposition both in present and future climate conditions was investigated in three perturbation experiments in the open Mediterranean Sea. Climate reactors (300 L) were filled with surface water collected in the Tyrrhenian Sea, Ionian Sea and in the Algerian basin during a cruise conducted in the frame of the PEACETIME project in May/June 2017. The experiments comprised two unmodified control tanks, two tanks enriched with a Saharan dust analog and two tanks enriched with the dust analog and maintained under warmer (+3 ºC) and acidified (-0.3 pH unit) conditions. Samples for the analysis of an extensive number of biogeochemical parameters and processes were taken over the duration (3-4 d) of the experiments. Dust addition led to a rapid release of nitrate and phosphate, however, nitrate inputs were much higher than phosphate. Our results showed that the impacts of Saharan dust deposition in three different basins of the open Northwestern Mediterranean Sea are at least as strong as those observed previously, all performed in coastal waters. The effects of dust deposition on biological stocks were different for the three investigated stations and could not be attributed to differences in their degree of oligotrophy but rather to the initial metabolic state of the community. Ocean acidification and warming did not drastically modify the composition of the autotrophic assemblage with all groups positively impacted by warming and acidification. Although autotrophic biomass was more positively impacted than heterotrophic biomass under future environmental conditions, a

Deleted: stratification

Deleted: Yet, w

Deleted: through

Deleted: in May/June 2017

Deleted: al protocol

Deleted: (3-4 d)

Deleted: Here, we present the general setup of the experiments and the impacts of dust seeding with and without addressing the effects of environmental changes on nutrients and biological stocks.

Deleted: and maximum input of nitrate whereas phosphate

Deleted: from the dust analog was much smaller

Deleted: However, interestingly, t

Deleted: highly

Deleted: between

stronger impact of warming and acidification on mineralization processes suggests a decreased capacity of Mediterranean surface plankton communities to sequester atmospheric CO_2 following the deposition of atmospheric particles.

1. Introduction

Atmospheric deposition is well recognized as a significant source of micro- and macro-nutrients for surface waters of the global ocean (Duce et al., 1991; Jickells et al., 2005; Moore et al., 2013). The potential modulation of the biological carbon pump efficiency and the associated export of carbon by atmospheric deposition events are still poorly understood and quantified (Law et al., 2013). This is especially true for Low Nutrient Low Chlorophyll (LNLC) areas where atmospheric fluxes can play a considerable role in nutrient cycling and that represent 60% of the global ocean surface area (Longhurst et al., 1995) as well as 50% of global carbon export (Emerson et al., 1997). These regions are characterized by low availability of macronutrients (N, P) and/or micronutrients (trace metals, in particular Fe) that can severely limit or co-limit phytoplankton growth during large periods of year.

The Mediterranean Sea is a typical example of these LNLC regions with overall surface chlorophyll *a* concentrations below 0.2 µg L^{-1} all year round, except in the Ligurian Sea where relatively large blooms can be observed in late winter-early spring (Mayot et al., 2016). Recent estimates indicate that the atmospheric input of nutrients in the Mediterranean Sea is within the same order of magnitude as riverine inputs (Powley et al., 2017), and, therefore, a considerable external source of nutrients (Richon et al., 2018). Atmospheric deposition originates both from natural (mainly Saharan dust) and anthropogenic sources (e.g. Bergametti et al., 1989; Desboeufs et al., 2018). Dust deposition, mostly in the form of pulsed inputs, is mainly associated with wet deposition (Loÿe-Pilot and Martin, 1996). Ternon et al. (2010) reported an average annual dust flux over four years of 11.4 g m^{-2} yr^{-1} (average during the period 2003–2007) at the DYFAMED station in the Northwestern Mediterranean Sea. In this region, the most important events reported in the 2010 decade amounted to ~22 g m^{-2} (Bonnet and Guieu, 2006; Guieu et al., 2010b).

Deleted: a

Deleted: metal

Deleted: e.g.

Deleted: and exhibits

Deleted: over most of its area

Deleted: assessments

Deleted: showed

Deleted: of

Deleted: making the atmosphere

Atmospheric deposition provides new nutrients to surface waters (Guieu et al., 2010b; Kouvarakis et al., 2001; Markaki et al., 2003; Ridame and Guieu, 2002), Fe (Bonnet and Guieu, 2006) and other trace metals(Desboeufs et al., 2018; Guieu et al., 2010b; Theodosi et al., 2010), representing significant inputs likely supporting primary production in particular during the period of stratification in spring/summer (Bonnet et al., 2005; Ridame and Guieu, 2002), although no direct correlation between dust and ocean color could be found from long series of satellite observation in that part of the Mediterranean basin (Guieu and Ridame, 2020).

Previous micro- and mesocosm experiments have shown that wet dust deposition events in the Northwestern Mediterranean Sea (the dominant deposition mode in that basin) are a stronger source of bioavailable nutrients compared to dry deposition. Wet deposition provides both new N and P while dry deposition supplies primarily P and, in contrast to wet deposition, does not stimulate the growth of the autotrophic community with the exception of diazotrophs (Ridame et al., 2013), resulting in no significant increase in chlorophyll *a* concentrations and primary production (Guieu et al., 2014a). In addition, wet dust deposition also modifies the bacterial assemblage leading to even stronger enhancements of heterotrophic production and respiration rates (Pulido-Villena et al., 2014). The carbon budget established from four artificial seeding experiments during the DUNE project (Guieu et al., 2014a) showed that by stimulating predominantly heterotrophic bacteria, atmospheric wet dust deposition can enhance the heterotrophic behavior of these oligotrophic waters. This has the potential to reduce organic carbon export to deep waters during the winter mixing period (Pulido-Villena et al., 2008) and ultimately limit net atmospheric CO_2 drawdown.

Conversely, the deposition of lithogenic particle from Saharan dust can promote aggregation and ballast organic matter leading to enhanced vertical export of organic carbon (Bressac et al., 2014; Desboeufs et al., 2014; Louis et al., 2017a; Ternon et al., 2010). These lithogenic processes can represent a major part of the carbon export following a dust deposition

Deleted: the

Deleted: that

Deleted: the

Deleted: especially

Deleted: stratification

Deleted: clear

Deleted: evidenced

Deleted: Experimental

Deleted: approaches

Deleted: present a higher impact as a

Deleted: fertilizing

Deleted: Indeed, w

Deleted: only

Deleted:

Deleted: allow to

Deleted: the autotrophic community

Deleted: This so-called fertilizing effect has been experimentally shown using both micro- and mesocosms where the wet deposition of Saharan dust analog strongly stimulated primary production and phytoplankton biomass (Guieu et al., 2014a; Ridame et al., 2014) while also modifying phytoplankton diversity (Giovagnetti et al., 2013; Lekunberri et al., 2010; Romero et al., 2011). In addition, besides phytoplankton,

Deleted: modified

Deleted: also

Deleted: community

Deleted: and led

Deleted: /or

Deleted: biological

Deleted: the fraction of

Deleted: that can be exported

Deleted: Another effect induced by

Deleted: deposition is the export of particulate organic carbon (POC), as lithogenic particles

Deleted: e

Deleted: dissolved

Deleted: This so-called

Deleted: carbon pump

event (up to 50% during the DUNE experiment; Bressac et al., 2014). Recently, Louis et al. (2017a) showed that Saharan dust deposition can also trigger the abiotic formation of transparent exopolymeric particles (TEP), leading to the formation of organic-mineral aggregates, a formation process that is highly dependent on the quality and quantity of TEP-precursors initially present in seawater.

In response to ocean warming and increased stratification, nutrient cycling in the open ocean is being and will continue to be perturbed in the next decades with regionally variable impacts (IPCC, 2019). Overall, LNLC areas are expected to expand in the future (Irwin and Oliver, 2009; Polovina et al., 2008) due to thermal stratification related reduction of nutrients supply from sub-surface waters (Behrenfeld et al., 2006). As such, the role of atmospheric deposition as a source of new nutrients to surface waters might increase. Ongoing warming and acidification (IPCC, 2019) are also evidenced in the Mediterranean Sea (e.g. Kapsenberg et al., 2017; The Mermex group, 2011). Whether or not plankton communities will respond differently to dust deposition in future conditions is still largely unknown. Although dependent on resource availability, it is well known that remineralisation by bacteria is subject to positive temperature control (López-Urrutia and Morán, 2007). Given that warming has no effect on primary productivity when plankton communities are nutrient limted (Marañón et al., 2018), temperature increase will most likely further push the balance towards net heterotrophy in oligotrophic areas.

In contrast, an *in situ* mesocosm experiment conducted during the summer stratification period in the Northwestern Mediterranean Sea showed that the plankton community was not sensitive to ocean acidification under strong nutrient limitation (Maugendre et al., 2017, and references therein). A batch experiment (Maugendre et al., 2015) showed that, under nutrient-depleted conditions in late winter, ocean acidification has a very limited impact on the plankton community and that small species (e.g. Cyanobacteria) might benefit from warming with a potential decrease of the export and energy transfer to higher trophic levels. In contrast, in more

Deleted: s

Deleted: resulting very likely in

Deleted: a

Deleted: might increase

Deleted: an alternative

Deleted: of the global ocean

Deleted: As under severe nutrient limitation,

Deleted: it

Deleted: With respect to ocean acidification,

Deleted: stratified

Deleted: rather

Deleted: insensitive

Deleted: this perturbation

Formatted: French

Deleted: This is coherent with results from Maugendre et al. (2015), based on a batch experiment,

Deleted: in

Deleted: g

Formatted: French

Field Code Changed

eutrophic (coastal) conditions, Sala et al. (2016) showed that ocean acidification had a positive effect on phytoplankton, especially on the pico and nano size classes. Similarly, Neale et al. (2014) showed that ocean acidification could lead to enhanced chlorophyll levels under low light conditions with an opposite effect under high irradiance, in coastal communities of the Alboran Sea.

To date and to the best of our knowledge, there have been no attempts to evaluate the behavior of plankton communities influenced by atmospheric deposition in the context of future temperature and pH changes. Such experiments were, therefore, conducted in the framework of the PEACETIME project (ProcEss studies at the Air-sEa Interface after dust deposition in the MEditerranean sea; http://peacetime-project.org/) on board the R/V "Pourquoi Pas?" during May/June 2017. The project aimed at studying and parameterizing the chain of processes occurring in the Mediterranean Sea driven by atmospheric deposition events including under on-going environmental changes (Guieu et al., 2020). During the cruise, three perturbation experiments were conducted in climate reactors (300 L tanks) filled with surface water collected in the Tyrrhenian Sea (TYR), Ionian Sea (ION) and Algerian basin (FAST; Fig. 1). Six tanks were used to follow simultaneously and with a high temporal resolution, the evolution of biological activity and stocks, nutrients, dissolved organic matter as well as particles dynamics and export, following a dust deposition event simulated, both under present environmental conditions and under a realistic climate change scenario for 2100 (ca. +3 °C and -0.3 pH units; IPCC, 2013). In this manuscript, we will present the general setup of the experiments and the evolution of nutrient and plankton communities (heterotrophic and autotrophic prokaryotes, photosynthetic eukaryotes as well as micro- and meso-zooplankton). Other manuscripts, related to these experiments in this special issue, focus on plankton metabolism (primary production, heterotrophic prokaryote production) and carbon export (Gazeau et al., 2021), microbial food

Deleted: exerted

Deleted: -

Deleted: -phytoplankton

Deleted: in a coastal ecosystem of the Alboran Sea

Deleted: ,

Deleted: although moderately,

Deleted: high

Deleted: after the deposition of

Deleted:

Deleted: particles

Deleted: levels of

Deleted: Yet, following the recommendation from Maugendre et al. (2017), any perturbation experiment for future climate conditions in the Mediterranean Sea should consider atmospheric deposition as a source of new nutrients and consider both temperature and pH as external forcings.

Deleted: during the cruise

Deleted: in

Deleted: extensively

Deleted: after

Deleted: and to put them in perspective of

Deleted: that

Deleted: in the

Deleted: stocks

Deleted: at their surface

Deleted: following

Deleted: biological stocks

Deleted: Several o

Deleted: and currently submitted to or published

Deleted: (Gazeau et al., 2021)

Deleted: on the

web (Dinasquet et al., 2021), nitrogen fixation (Céline Ridame, unpublished results) and on the release of insoluble elements (Fe, Al, REE, Th, Pa) from dust (Roy-Barman et al., 2021).

Deleted:
Deleted: (Dinasquet et al., 2021)
Deleted: on
Deleted: 0

2. Material and Methods

2.1. General setup

Six experimental tanks (300 L; Fig. 2), in which the irradiance spectrum and intensity can be finely controlled and future ocean acidification and warming conditions can be fully reproduced, were installed in a temperature-controlled container. The tanks are made of trace-metal free high-density polyethylene (HDPE), with a height of 1.09 m, a diameter of 0.68 m, a surface area of 0.36 m^2 and a volume of 0.28 m^3. Each tank was equipped with a lid containing six rows of LEDs (Alpheus©). Each of these rows were composed of blue, green, cyan and white units in order to mimic the natural sun spectrum. At the conical base of each tank, a polyethylene (PE) bottle was screwed onto a polyvinyl chloride (PVC) valve that remained open during the duration of the whole experiment to collect the sinking material. Photosynthetically active radiation (PAR; 400-700 nm) and temperature were continuously monitored in each tank using respectively QSL-2100 Scalar PAR Irradiance Sensors (Biospherical Instruments©) and pt1000 temperature sensors (Metrohm©) connected to a D230 datalogger (Consort©).

Prior to the start of the experiments, tanks were cleaned following the protocol described by Bressac and Guieu (2013). Three sets of experiments were carried out at the long duration stations ION, TYR and FAST, respectively, and comprised two unmodified control tanks (C1 and C2), two tanks enriched with Saharan dust (D1 and D2) and two tanks enriched with Saharan dust and maintained under warmer (+3 ºC) and acidified (-0.3 pH unit) conditions (G1 and G2). The atmosphere above tanks C1, C2, D1 and D2 was flushed with ambient air (ca. 400 ppm, 6 L min^{-1}) and tanks G1 and G2 were flushed with air enriched with CO_2 (ca. 1000 ppm, 6 L min^{-1}) in order to prevent CO_2 degassing from the acidified tanks. CO_2 partial pressure (pCO_2) in both ambient air and CO_2-enriched air was monitored using two gas analysers (LI-820, LICOR©).

Deleted: in which

Deleted: and are trace-metal free in order to avoid contaminations,

Deleted: All tanks were cleaned before the experimental work following the protocol described by Bressac and Guieu (2013). A weak turbulence was generated by a rotating PVC blade (9 rpm) in order to mimic natural conditions.

Deleted: collecting the exported material from above

Deleted: The experimental protocol

The CO_2 concentration in the CO_2-enriched air was manually controlled through small injections of pure CO_2 (Air Liquide©) using a mass flow controller. Mixing in the tanks was ensured by a rotative PVC blade (9 rpm) mimicking natural turbulence

The tanks were filled by means of a peristaltic pump (Verder© VF40 with EPDM hose, flow of 1200 L h^{-1}) collecting seawater below the base of the boat at around 5 m, used to supply continuously surface seawater to a series of instruments during the entire campaign. In order to homogeneously fill the tanks, the flow was divided into six HDPE pipes distributing the water simultaneously into the different tanks. The procedure was started at the end of the day at all three stations and took approximately 2 h (including rinsing and initial sampling. While filling the tanks, samples were taken for the measurements of selected parameters (sampling time = t-12h before dust seeding; Table 1). After filling the tanks, seawater in tanks G1 and G2 was slowly warmed overnight using 500 W heaters, controlled by temperature-regulation units (COREMA©), to reach an offset of +3 °C. ^{13}C-bicarbonate was added to all tanks at 4:00 am (local time; Gazeau et al., 2021) and at 4:30 am G1 and G2 were acidified by addition of CO_2-saturated filtered (0.2 µm) seawater (~1.5 L in 300 L; collected when filling the tanks at each station) to reach a pH offset of -0.3. Further samples for a range of parameters were taken (sampling time = t0, Table 1), followed by dust seeding carried out between 7:00 and 9:00 (local time) in tanks D1, D2, G1 and G2. The same dust analog flux was applied as in the DUNE 2009 experiments described in Desboeufs et al. (2014). The dust was derived from the <20 µm fraction of soil collected in Southern Tunisia (a major source for material transported and deposited in the Northwestern Mediterranean) consisting of quartz (40%), calcite (30%) and clay (25%) with most particles (99%) smaller than 0.1 µm (Desboeufs et al., 2014). The collected material underwent an artificial chemical aging process by addition of nitric and sulfuric acid (HNO_3 and H_2SO_4, respectively) to mimic cloud processes during atmospheric transport of aerosol with anthropogenic acid gases (Guieu et al., 2010a, and references therein). To mimic a

Deleted: Three experiments were performed at the long duration stations TYR, ION and FAST.

Formatted: Space After: 0 pt, Border: Top: (No border), Bottom: (No border), Left: (No border), Right: (No border), Between : (No border)

Deleted: large

Deleted: (depth of

Deleted: ~

Deleted:)

Deleted: Overall,

Deleted: the filling of the six tanks

Deleted: ~

Deleted: , see thereafter). At the three stations, tanks were always filled at the end of the day before the start of the experiments: TYR (17/05/2017), ION (25/05/2017) and FAST (02/06/2017). …

Deleted: this surface seawater was sampled

Deleted: , see

Deleted: in G1 and G2 overnight

Deleted: at 4:30 am

Deleted: S

Deleted: ing

Deleted: most

Deleted: took place

Deleted: prior to dust seeding

Deleted: see

Deleted: . D

Deleted: was performed right after t0

Deleted: was used and the same dust

Deleted: simulated

Deleted: for

Deleted: Briefly, the fine fraction (< 20 µm) of Saharan soils collected in southern Tunisia, which is a major source of dust deposition over the northwestern Mediterranean basin, was used in the seeding experiments. The particle size distribution showed that 99% of particles had a size smaller than 0.1 µm, and that particles were mostly made

Deleted: This

Deleted: dust

realistic wet flux event for the Mediterranean of 10 g m^{-2}, 3.6 g of this analog dust were quickly diluted in 2 L ultrahigh-purity water (UHP water; 18.2 MΩ cm^{-1} resistivity), and sprayed at the surface of the tanks using an all-plastic garden sprayer (duration = 30 min). The total N and P mass in the dust were 1.36 ± 0.09% and 0.055 ± 0.003%, respectively (see Desboeufs et al., 2014, for a full description of dust chemical composition). Biogeochemical parameters and processes measured during the experiments are listed in Table 1. The experiment lasted 3 days (72 h) at stations TYR and ION and 4 days (96 h) at station FAST, as constrained by the time available between stations. Seawater sampling was conducted 1 h (t1h), 6 h (t6h), 12 h (t12h), 24 h (t24h), 48 h (t48h) and 72 h (t72h) after dust additions in all three experiments with an additional sample after 96 h (t96h) at FAST). Acid-washed silicone tubes were used for transferring the water collected by gravity from the tanks to the different vials or containers.

2.2. Analytical methods

2.2.1. Carbonate chemistry

Seawater samples for pH measurements were stored in 300 mL glass bottles with a glass stopper, pending analysis on board (within 2 h). Samples were transferred to 30 mL quartz cells and absorbances at 434, 578 and 730 nm were measured at 25 °C on an Cary60 UV-Spectrophotometer (Agilent©) before and after addition of 50 µL of purified meta-cresol purple provided by Robert H. Byrne (University of South Florida, USA) following the method described by Dickson et al. (2007). pH on the total scale (pH_T) was computed using the formula and constants of Liu et al. (2011). The accuracy of pH measurements (0.007 pH units) was estimated using a TRIS buffer solution (salinity 35, provided by Andrew Dickson, Scripps university, USA).

Deleted: to

Deleted: of

Deleted: total contents

Deleted: of N

Deleted: of P

Deleted: The experimental protocol included the analysis of an extensive number of b

Deleted: , not all shown and discussed in this paper,

Deleted: and

Deleted: lasted 72 h (3 days) whereas the last experiment

Deleted:

Deleted: was extended to four days. This relatively short duration of the experiments was

Deleted: and the time needed to properly clean the tanks between the experiments, following the protocol described by Bressac and Guieu (2013). As a larger time window was possible at the end of the cruise, the experiment at FAST was extended to four days.

Formatted: English (US)

Deleted: + 96 h =

Deleted: for station

Deleted: after dust addition

Deleted: For some parameters (e.g. micro- and macro-nutrients), sampled seawater was directly filtered at the exit of the sampling tubes connected to each tank on sterile membrane filter capsules (gravity filtration with Sartobran© 300; 0.2 µm).

Formatted

Deleted: to 0.007 pH units,

Seawater samples (500 mL) for total alkalinity (A_T) measurements were filtered on GF/F membranes and analyzed onboard within one day. A_T was determined potentiometrically using a Metrohm© titrator (Titrando 888) and a glass electrode (Metrohm©, ecotrode plus) calibrated using first NBS buffers (pH 4.0 and pH 7.0, to check that the slope was Nernstian) and then using a TRIS buffer solution (salinity 35, provided by Andrew Dickson, Scripps university, USA). Triplicate titrations were performed on 50 mL sub-samples at 25 ºC and A_T was calculated as described by Dickson et al. (2007). Titrations of standard seawater provided by Andrew Dickson (Scripps university, USA; batch 151) yielded A_T values within 5 µmol kg^{-1} of the nominal value and a standard deviation of 1.5 µmol kg^{-1} (n = 40).

All parameters of the carbonate chemistry were determined from pH_T, A_T, temperature, salinity, as well as phosphate and silicate concentrations using the R package seacarb. Propagation of errors on computed parameters was performed using the new function "error" of this package, encompassing errors associated with the estimation of A_T, pH_T as well as errors on the dissociation constants (Orr et al., 2018).

2.2.2. Nutrients

Seawater samples for dissolved nutrients were collected in polyethylene bottles after passage through sterile membrane filter capsules (Sartobran″ 300; 0.2 µm) connected to the sampling tubes of each tank (Sartobran© 300; 0.2 µm), and analyzed directly on board. Nitrate + nitrite (NO_x) and silicate ($Si(OH)_4$) measurements were conducted using a segmented flow analyzer (AAIII HR Seal Analytical©) according to Aminot and Kérouel (2007) with a detection limit of 0.05 µmol L^{-1} for NO_x and 0.08 µmol L^{-1} for $Si(OH)_4$. In addition, at t-12h, NO_x was also analysed by spectrometry at 540 nm, with a 1 m Liquid Waveguide Capillary Cell (LWCC), with a detection limit of ~10 nmol L^{-1} and the reproducibility was ~6%. Ammonium concentrations in samples from t-12h were also measured on board using a Fluorimeter TD-700

Deleted: ; 500 mL

Deleted: (

Deleted: =

Deleted: ,

Deleted: considering

Deleted: filtered directly at the exit of the

Deleted: connected to

Deleted: collected in polyethylene bottles

Deleted: immediately

Deleted: of quantification

Deleted: for

Deleted: samples

Deleted: the analysis of

Deleted: performed

Deleted: a

Deleted: ic

Deleted: method in the visible

Deleted: . The

Deleted: of detection was

Deleted: Also from samples taken at t-12h, the measurement of a…

Deleted: was performed

(Turner Designs©) according to Holmes et al. (1999). This later method is based on the reaction of ammonia with orthophtaldialdehyde and sulfite and has a detection limit of 0.01 µmol L^{-1}. Dissolved inorganic phosphorus (DIP) concentrations were quantified using the Liquid Waveguide Capillary Cell (LWCC) method according to Pulido-Villena et al. (2010). The LWCC was 2.5 m long and the detection limit was 1 nmol L^{-1}.

Deleted: fluorimetric

Deleted: of quantification

Deleted: of detection

Formatted: English (UK)

2.2.3. Pigments

For pigment analysis, 2.5 L seawater from the tanks were filtered onto GF/F filters, immediately frozen in liquid nitrogen and stored at -80 ºC pending analysis at the SAPIGH analytical platform at the Institut de la Mer de Villefranche (IMEV, France). Filters were sonicated at -20 ºC in 3 mL methanol (100%) containing an internal standard (vitamin E acetate, Sigma©) and clarified one hour later by vacuum filtration through GF/F filters. The extracts were rapidly analyzed (within 24 h) on a complete Agilent© Technologies 1200 series HPLC system. The pigments were separated and quantified as described in Ras et al. (2008).

Deleted: A volume of

Deleted: of sampled

Deleted: was

Deleted: extracted

Deleted: , disrupted by sonication

2.2.4. Flow cytometry

For flow cytometry, samples (4.5 mL) were fixed with glutaraldehyde grade I (1% final concentration), and incubated for 30 min at 4 °C, quick-frozen in liquid nitrogen and stored at -80 °C until analysis. Samples were thawed at room temperature. Counts were performed on a FACSCanto II flow cytometer (Becton Dickinson©) equipped with 3 air-cooled lasers: blue (argon 488 nm), red (633 nm) and violet (407 nm). Following Marie et al. (2010), *Synechococcus* spp. was discriminated by its strong orange fluorescence (585 ± 21 nm), and autotrophic pico- and nano-eukaryotes were discriminated by their scatter signals of red fluorescence (> 670 nm). For the enumeration of heterotrophic prokaryotes, cells were stained with SYBR Green I (Invitrogen – Molecular Probes) at 0.025% (vol / vol) final concentration for

Deleted: the enumeration of autotrophic prokaryotic and eukaryotic cells, heterotrophic prokaryotes and heterotrophic nanoflagellates (HNF) by

Deleted: sub

Deleted: 25%

Deleted: then

Deleted: The separation of different autotrophic populations was based on their scattering and fluorescence signals according to…

Deleted: .

15 min at room temperature in the dark. Stained prokaryotic cells were discriminated and enumerated according to their right-angle light scatter (SSC) and green fluorescence at 530/30 nm. Heterotrophic prokaryotes were distinguished from autotrophic prokaryotes based on the green vs. red fluorescent signal. The same procedure was used for the enumeration of HNF, after staining with 0.05% (v/v) final SYBR Green I concentration for 15-30 min at room temperature in the dark (Christaki et al., 2011). Fluorescent beads (1.002 µm; Polysciences Europe©) were systematically added to all samples as internal standard. Cell concentrations were determined based on counts and flow rate, estimated with TruCount beads (BD biosciences©). Biomass of each group were estimated based on conversion equations and/or factors found in the literature (see section 2.3.2).

2.2.5. Micro-phytoplankton and -heterotrophs

At t-12h, 500 mL samples were collected in glass vials and immediately preserved with 5% final concentration acidic Lugol's solution. Back at the Laboratoire d'Océanographie de Villefranche (LOV, France), 100 mL aliquots were transferred to sedimentation chambers (Utermohl) and counted under an inverted microscope at x 200 to x 400 magnification.

2.2.6. Mesozooplankton

At the end of each experiment, the sedimentation bottles were removed, fixed with formaldehyde 4% (see Gazeau et al., 2021) and stored for analysis back in the home laboratory. Subsequently, the valve at the base of each tank, that allowed retrieval of the sedimentation bottles without disturbance, was opened, the remaining water inside the tanks (165-180 L at TYR; 172.5 L at ION and 150 L at FAST) as filtered through a 100 µm mesh size PVC sieve. The organisms retained were gently removed using a washing bottle filled with filtered seawater (0.2 µm), and transferred directly in a 250 mL bottle and fixed with 4% final concentration

Deleted: In a plot of green versus red fluorescence, h
Deleted: . F
Formatted: English (US)
Deleted: was performed
Deleted: (Invitrogen—Molecular Probes) at 0.05% (v/v) final concentration
Deleted: Cells were discriminated and enumerated ... [1]
Deleted: each
Deleted: analyzed
Deleted: The c
Deleted: abundance
Deleted: was
Deleted: from the
Deleted: which was calculated
Deleted: es
Formatted ... [2]
Deleted: (i.e. seawater sampled during the filling of th ... [3]
Deleted: a volume of
Deleted: was sampled
Deleted: in a
Deleted: pending analysis
Deleted: At
Deleted: s
Deleted: (t+72h for TYR and ION and t+96 h for FAS ... [4]
Deleted: traps
Deleted: , closed and stored
Formatted ... [5]
Deleted: T
Deleted: the
Formatted ... [6]
Deleted: s
Deleted: then re
Deleted: to let
Deleted: TYR
Deleted: ION =
Deleted: FAST =
Deleted:)
Deleted: pass
Deleted: large
Deleted: (100 µm)
Deleted: on that mesh
Deleted: from the sieve
Deleted: side
Deleted: . The bottle was filled with the sample (1/3 o ... [7]

formaldehyde. These samples were processed using a ZooSCAN (Hydroptic©; Gorsky et al., 2010) at the PIQv-platform of EMBRC-France. Organisms were identified and counted using automatic classification with a reference dataset in EcoTaxa (https://ecotaxa.obs-vlfr.fr/, last access: 17/04/2020), followed by manual validation.

2.3. Data analyses

2.3.1. Nutrient inputs from dust

The maximum percentage of dust-born dissolved N and P was estimated based on initial N and P composition of the dust analog (see section 2.1; Desboeufs et al., 2014) and maximal concentrations observed in tanks D and G at t1h and t6h after seeding, as follows:

$$\%_{dissolution} = \frac{CONC_{max} - CONC_{init}}{CONC_{dust}} . 100 \quad (1)$$

where $CONC_{init}$ is the concentration of the corresponding nutrient in each tank before seeding (t0), $CONC_{max}$ corresponds to the concentration of the corresponding nutrient in each tank when nutrient concentration was at a maximum within the first 6 h after seeding, and $CONC_{dust}$ is the maximum potential concentration, assuming a 100% dissolution from dust analog (based on dust content; Desboeufs et al. 2014; section 2.1).

2.3.2. Autotrophic and heterotrophic biomass

Given that samples for micro-phytoplankton counts were taken only at t-12h, as a first approximation, autotrophic biomass was estimated as the sum of *Synechococcus*, autotrophic pico-eukaryotes and nano-eukaryotes biomass (based on flow cytometry). Conversion of abundances to to carbon units was carried out assuming 250 fg C $cell^{-1}$ *for Synechococcus* (Kana and Glibert, 1987). The biovolume to carbon content relationship of Verity et al. (1992) was used

Deleted: The zooplankton digital images
Deleted: were obtained
Deleted: The identification of species
Deleted: was performed
Deleted: by
Deleted: and then a
Deleted: ll validated and corrected manually.
Formatted: Font colour: Auto,
Deleted: calculated
Deleted: considering that these evapo-condensated dust contain 1.36 ± 0.09% of N and 0.055 ± 0.003% of P (Desboeufs et al., 2014). B
Formatted: English (US)
Deleted: the
Deleted: tanks after seeding (two discrete sampling within 6 h following dust seeding,
Deleted:)
Deleted: one can estimate the maximal % of dissolution of dust in seawater during the three experiments
Deleted: over
Deleted: as observed based on our discrete sampling procedure…
Deleted: addition
Deleted: corresponding
Deleted: to
Deleted: of its total concentration in
Deleted: the
Deleted: 3/25/21 4:05:00 PM
Deleted: As
Deleted: counting
Deleted: was not performed throughout the experiment
Deleted: calculated
Deleted: carbon contained in
Deleted: abundances
Deleted: and is therefore restricted to the fraction < 20 µm
Deleted: For *Synechococcus*,
Deleted: c
Deleted: done considering
Formatted: Font: Italic
Deleted: , while the equation proposed by

for autotrophic pico- and nano-eukaryotes assuming a spherical shape and a diameter of 2 and 6 µm, respectively. Heterotrophic biomass was computed as the sum of heterotrophic prokaryotes (HP) biomass and heterotrophic nanoflagellates (HNF) biomass. Conversion to carbon biomass were done assuming 20 fg C $cell^{-1}$ (Lee and Fuhrman, 1987) for heterotrophic prokaryotes and 220 fg C μm^{-3} (Børsheim and Bratbak, 1987) with a spherical shape and 3 µm diameter for heterotrophic nanoflagellates. The ratio of autotrophic and heterotrophic biomass during the experiments was used to evaluate the trophic status of the investigated communities and its evolution. Finally, a proxy for micro-phytoplankton biomass (B_{micro}) was estimated following Vidussi et al. (2001), as the sum of Fucoxanthin and Peridinin.

Deleted: for the two groups

Deleted: Percentages of these different groups were calculated in order to estimate the composition of the communities at the start and its evolution during the experiments. Furthermore, h

Deleted: For heterotrophic prokaryotes,

Deleted: c

Deleted: units

Deleted: considering

Deleted: for heterotrophic nanoflagellates assuming

Deleted: ,

Deleted: a diameter of

3. Results

3.1. Initial conditions

Initial conditions at the three sampling stations while filling the tanks (t-12h before seeding) are shown in Table 2. pH_T, total alkalinity concentrations increased from west to east (Table 2). NO_x and DIP concentrations followed different patterns with highest NO_x values at station FAST and highest DIP concentrations at station TYR. Consequently, the lowest NO_x:DIP ratio was measured at TYR (0.8), compared to ION and FAST (2.8 and 4.6, respectively). Ammonium concentrations ranged between 0.045 µmol L^{-1} to below detection limit at FAST. Silicate concentrations were similar at stations TYR and ION (~ 1 µmol L^{-1}) and higher than at station FAST (0.64 µmol L^{-1}).

Very low chlorophyll *a* concentrations were measured at the three stations (0.063 - 0.072 µg L^{-1}). The proportion of the different major pigments (Fig. 3) indicates that phytoplankton communities were similar with a dominance of Prymnesiophytes (i.e. 19'-hexanoyloxyfucoxanthin; Ras et al., 2008) followed by Cyanobacteria (i.e. Zeaxanthin; Ras et al., 2008) at stations TYR and ION. In contrast, at station FAST, the plankton community was clearly dominated by photosynthetic prokaryotes (i.e. Zeaxanthin and Divinyl-chlorophyll *a* as proxies for Cyanobacteria and Prochlorophytes, respectively; Ras et al., 2008). At all three stations, the proportion of pigments representative of larger species (i.e. Fucoxanthin and Peridinin; diatoms and dinoflagellates respectively; Ras et al., 2008) were very small (< 5%).

At all stations, autotrophic nanoplankton contributed most to total biomass. Autotrophic and heterotrophic biomass and abundances were highest at station FAST, followed by ION for the autotrophs and TYR for heterotrophs (Table 2). Differences in standing stocks between stations where more pronounced for the heterotrophs. As a consequence, the ratio between

Deleted: of various measured parameters

Deleted: and

Deleted: followed a

Deleted: increasing gradient (8.03, 8.04 and 8.07; 2443, 2529 and 2627 µmol kg^{-1} at FAST, TYR and ION, respectively)…

Formatted: Subscript

Deleted: concentrations were maximal at station FAST with a NO_x:DIP molar ratio of ~ 4.6. Very low NO_x concentrations were observed at stations TYR and ION (14 and 18 nmol L^{-1}, respectively). DIP concentrations were the highest at station TYR (17 nmol L^{-1}) and the lowest at the most eastern station (ION, 7 nmol L^{-1}).

Deleted: were maximal at TYR

Deleted: (

Deleted:), intermediate at ION (0.022 µmol L^{-1}), and minimal at FAST

Deleted: (

Deleted:)

Deleted: and similar concentrations of

Deleted: showed

Deleted: at stations TYR and ION

Deleted: very

Formatted: English (US)

Formatted: Font: Italic

Deleted: for each pigment

Deleted: Cellular abundances of all studied microorganisms (phytoplankton, micro-grazers, heterotrophic bacteria) were the highest at FAST (Table 2). Picoeukaryotes, *Synechococcus* and heterotrophic prokaryotes abundances followed an east to west increasing trend (ION < TYR < FAST). In contrast, nano-eukaryotes abundance was similar at FAST and ION, and minimal at TYR. The abundance of heterotrophic nanoflagellates (HNF) were similar at TYR and FAST (~110-125 cells mL^{-1}), twice as high as the one observed at station ION. This east to west increasing trend was also observed for micro-phytoplankton and micro-heterotrophs abundances (microscopic analyses; Table 2). T

autotrophic biomass and heterotrophic biomass ranged from ~0.6 at TYR and FAST to 1.3 at ION.

3.2. Conditions of irradiance, temperature and pH during the experiments

Irradiance levels during the experiments are shown in Fig. 4. Decrease in water transparency after dust addition was observed at all three stations with the lowest impact at station FAST where irradiance levels decreased by only 60 µmol photons m^{-2} s^{-1} after dust addition, reaching similar levels as observed for tanks D and G. At station TYR, a more pronounced decrease was observed in acidified and warmed tanks (G1 and G2) with a decrease of daily average maximum irradiance of ~ 60 and ~ 160 µmol photons m^{-2} s^{-1} compared to dust-amended tanks D and controls, respectively. Temperature control (Fig. 4) was not optimal showing deviations between replicates of treatment G of up to 1.0 °C (station FAST). Temperature in controls and D tanks displayed a daily cycle, increasing during the day and decreasing at night (Fig. 4). The differences between the warmed treatment (G) and the other tanks were +3, +3.2 and +3.6 °C at TYR, ION and FAST, respectively.

Addition of CO_2-saturated filtered seawater led to a decrease in pH_T from 8.05 ± 0.004 (average ± SD of C1, C2, D1 and D2 at t0) to 7.74 (average between G1 and G2) at station TYR, from 8.07 ± 0.002 to 7.78 at station ION and from 8.05 ± 0.001 to 7.72 at station FAST (Fig. 5). pH_T levels remained more or less constant in the control and D tanks during all three experiments with no clear impact of dust addition. In G tanks, pH levels gradually increased during the experiments with larger variability between duplicates. These increases remained moderate thanks to the flushing of CO_2-enriched air above the tanks (pCO_2 of 1017 ± 11, 983 ± 96, 1023 ± 25 ppm at TYR, ION and FAST, respectively; data not shown). Partial pressure of CO_2 in ambient air was 410 ppm, similar for the three stations. In all experiments, the addition of

Deleted: was clearly in favor of the heterotrophic compartment at stations TYR and FAST (
Deleted: at the two stations
Deleted:)
Deleted: but the opposite was found at station ION (ca.
Deleted:)
Deleted: ,
Deleted: in the control tanks (C1, C2), were maximal at station ION and minimal at station FAST (daily average maximum levels in controls: ~ 1050, ~ 1130 and ~ 1020 µmol photons m^{-2} s^{-1} at TYR, ION and FAST, respectively;
Deleted:)
Deleted: s
Deleted: of
Deleted: a maximum dust impact at station ION and
Deleted: (average between
Deleted:)
Deleted: as
Deleted: 5
Deleted: ION
Deleted: with an
Deleted: e
Deleted: a
Deleted: e
Deleted: Overall, t
Deleted: of
Deleted: between
Deleted: ambient pH levels
Deleted: in tanks D1 and D2
Deleted: lowered pH
Deleted: a systematic
Deleted: increase
Deleted: in one of the
Deleted: (G1)
Deleted: Yet pH_T
Deleted: at
Deleted: , i.e. 410 ppm (data not shown)
Deleted: At all three stations

^{13}C-bicarbonate led to an increase of total alkalinity between 6 and 11 µmol kg^{-1} at t0. Dust addition, right after t0 in tanks D and G, led to a A_T decrease between 8 and 16 µmol kg^{-1} at t24h with no apparent effects of warming and acidification. Overall, no large changes in A_T were observed during the experiments (Fig. 5).

3.3. Changes in nutrient concentrations

Dust addition led to a rapid increase in NO_x (~ 11 µmol L^{-1} as observed during the first 6 h; Fig. 6; Table 3) at all three stations with no differences between treatments D and G. The corresponding percent dissolution of N from dust ranged between 94 and 99%. In contrast, maximum DIP release was much smaller, ranging between 20 and 37 nmol L^{-1}, with slightly higher values at FAST (31-37 nmol L^{-1}) as compared to the other stations. Percent dissolution for DIP corresponded to 9.2 to 17.3% of total phosphorus contained in dust. As a consequence, NO_x:DIP ratios increased from initial values below 5 to above 300, within 6 h after dust seeding, in tanks D and G (Fig. 6).

After the rapid increase of N and P, both nutrients decreased with time. While nutrient variability was small in control tanks (NO_x and DIP variations below 20 and 3 nmol L^{-1}, respectively), large decrease in both elements occured in dust amended tanks (D and G; Table 4). Similar linear decrease in NO_x were observed throughout the experiments at stations TYR and ION with no visible differences between tanks D and G. In contrast, at station FAST, a more pronounced decrease in NO_x was observed in dust-amended (D and G) tanks, as well as in warmed and acidified tanks relative to the D treatment. Nevertheless, at all stations, NO_x concentrations in D and G treatments remained far above ambient levels throughout the experiments (> 9 µmol L^{-1}). Abrupt decreases in DIP were observed during the three experiments after the initial increase. At station TYR, after 24 h, all DIP released from dust decreased to initial levels in tanks G while it took two more days to reach initial levels in tanks D. In contrast,

Deleted: to all tanks before t0
Deleted: performed
Deleted: in these tanks
Deleted: this parameter
Deleted: in tanks D and G
Deleted: and maximum input of
Deleted: of ~ 11 µmol L^{-1}
Deleted: both
Deleted: percentage
Deleted: contained in the
Deleted: analog was
Deleted: (within 6 h after dust addition) from the dust analog …
Deleted: and comprised
Deleted: release
Deleted: D
Deleted: percentages
Deleted: were estimated between
Deleted: and
Deleted: of these contrasted dissolution of N and P
Deleted: the dust amended (
Deleted:) tanks
Deleted: se
Deleted: s
Deleted: due to
Deleted: releases in dust amended tanks
Deleted: variables
Deleted: over the duration of the experiments
Deleted: of
Deleted: was measured
Deleted: For NO_x, s
Deleted: s
Formatted: Subscript
Deleted: as compared to the other stations
Deleted: with detectable
Deleted: larger decreases

at station ION, no clear difference in DIP dynamics was observed between treatments D and G, with concentrations that decreased rapidly during the first 24 h but remained above initial levels until the end of the experiment. At station FAST, similarly to station TYR, DIP decreased rapidly from t12h in treatment G, reaching levels close to initial conditions at the end of the experiment. DIP decrease was much lower in treatment D (Table 4) with concentrations maintained far above ambient levels throughout the experiment. As a consequence of the differences between NO_x and DIP dynamics as well as differences among stations, NO_x:DIP ratio increased, with clear differences between stations (Fig. 6), and remained much higher than in the controls.

At all stations, silicate concentrations were higher in dust amended tanks relative to the controls. At TYR, while concentrations remained stable in control tanks, they increased linearly with time in the other tanks (D and G) with no apparent effect of the imposed increase in temperature and decrease in pH (i.e. tanks G). Difference in $Si(OH)_4$ concentrations between dust amended treatments (D and G) and controls was ~0.1 µmol L^{-1} at the end of the experiment. At station ION, after an initial decrease in concentrations between t-12h and t0, concentrations increased in all tanks until the end of the experiment with higher values in dust amended tanks (D and G) than in controls and no difference between D and G treatments. In contrast, at FAST, concentrations increased from t-12h to t48h (with higher values in dust amended tanks) and decreased onward until the end of the experiment. At the end of the experiment (t96h), $Si(OH)_4$ concentrations were higher in the G treatment than in the D treatment which were similar to the controls.

3.4. Changes in biological stocks

Temporal dynamics in biological parameters showed very different patterns at each station. At TYR, total chlorophyll *a* concentrations did not change in the dust amended D tanks

Deleted: that

Deleted: se

Deleted: during the experiments

Deleted: that

Deleted: over the duration of the three experiments

Deleted: S

Deleted: dynamics showed at all stations higher

Deleted: (D and G)

Deleted: of

Deleted: of

Deleted: concentration

Deleted: (

Deleted:)

Deleted: between

Deleted: and t0, and continued to increase in all tanks (with higher values in dust amended tanks) until

Deleted: then

Deleted: was

Deleted: was

Deleted: Regarding biological stocks, t

Deleted: amongst the three studied

Deleted: s

(Fig. 7) and even led to slightly decreased values 24 h after dust addition (e.g. -35 to -38% in D1 and D2, respectively as compared to controls; Table 5). No clear effects of dust addition (tanks D vs. C) were detectable for all groups based on pigment analyses (Fig. 7). Results obtained based on flow cytometry counts (Fig. 8) were coherent with these observations and showed stronger decreases in cell abundances for < 20 µm autotrophic groups in tanks D1 and D2 (-77 to -80%). In contrast, the abundance of heterotrophic prokaryotes (HP) increased rapidly after dust addition both under ambient (+53-68%) and future (+68%) environmental conditions, with no clear difference among treatments. In warmed and acidified tanks (G), strong discrepancies between the duplicates were observed for pigments and autotrophic cell abundances; tank G1 showed moderate increases for all variables with the exception of autotrophic pico-eukaryotes, while in G2 all variables responded strongly to dust addition with maximum relative changes of > 300%, with the exception of autotrophic nano-eukaryotes. While HNF abundances responded positively to the treatments in D1, D2 and G2, abundances increased sharply in tank G1 towards the end of the experiment.

At ION, clear differences between treatments were observed for almost all pigments and cell abundances (Fig. 7, Fig. 8). With the exception of autotrophic nano-eukaryotes and HNF, all variables (pigments and cell abundances) increased as a response to both dust addition and warmed/acidified conditions (Table 5). The maximum relative changes as compared to controls observed for total chlorophyll *a* were 109-183% and 399-426% in tanks D and G, respectively. The highest stimulation by dust addition was observed for *Synechococcus* with +317-390% and +805-1425% increase in abundances in D and G tanks respectively (Table 5). Autotrophic nano-eukaryotes and HNF abundances did not respond to dust addition under ambient conditions but an increase in abundances occured in treatment G. In contrast to observations at TYR, temperature and pH affected heterotrophic prokaryotes in all dust-amended tanks at station ION with a higher impact of dust addition under future environmental conditions.

Deleted: maintained under ambient levels of temperature and pH …

Deleted: counting

Deleted: , at this station

Deleted: those

Deleted: .

Deleted: Indeed,

Deleted: ly higher levels

Deleted: as compared to tanks C

Deleted: (

Deleted: : +119%)

Deleted: (+100-352%)

Deleted: (+1095%)

Deleted: a

Deleted: distinction

Deleted: could be

Deleted: (i.e. C < D < G). As an example

Deleted: ,

Deleted: the

Deleted: to

Deleted: a

Deleted: increase

Deleted: increase

Deleted: Abundances of

Deleted: suggested

Deleted: no impact of

Deleted: positive impact

Deleted: to what was observed

Deleted:

Deleted: for HP abundances

Deleted: an effect of

Deleted: was observed

Deleted:

At station FAST, all biological stocks increased strongly after dust addition (Fig. 7, Fig. 8 and Table 5). Total chlorophyll *a* increased following exponentially until the end of the experiment with slightly lower values observed under ambient environmental conditions (+237-318% in D tanks and ~ +400% in G tanks). Prymnesiophytes (i.e. 19'-hexanoyloxyfucoxanthin) and diatoms (i.e. Fucoxanthin) appeared as the groups benefiting the most from dust addition with no large impacts of warming/acidification while Pelagophytes (i.e. 19'-butanoyloxyfucoxanthin) and green algae (i.e. Total Chlorophyll *b*) showed a stronger response in treatment G. Finally, although Cyanobacteria (i.e. Zeaxanthin) responded faster to dust addition under future environmental conditions (tanks G), this effect attenuated towards the end of the experiment. In contrast to estimates based on pigments, increases in cell abundances did not generally last until the end of the experiments. While abundances of autotrophic pico-eukaryotes increased until t96h in treatment D, abundances sharply declined between t72h and t96h for this group in treatment G. The same trend was observed for *Synechococcus*, although discrepancies between duplicates in treatment D at t96h did not allow drawing conclusions on the behavior of this group by the end of the experiment. Abundances of autotrophic nano-eukaryotes declined sharply between t72h and t96h under present and future conditions. The decline in HP abundances occured earlier during the experiment with moderate maximum relative differences as compared to controls at t48h. HP abundances declined very sharply between t48h and t96h in treatment G, reaching control levels, while this decline was less sharp under present environmental conditions. Finally, HNF dynamics during this experiment was hard to interpret given the large increase in abundances in only one duplicate of treatment G (t24h) followed by a gradual decline.

Abundances of meso-zooplankton at the end of the experiments showed relatively similar values at stations TYR and ION while much higher levels were observed at station FAST (Fig. 9). As a consequence of large variability between duplicates at stations TYR and ION, no clear

Deleted: above mentioned variables related to

Deleted: For instance, t

Deleted: an

Deleted: trend

Deleted: reaching maximal values at t96h

Deleted: vs.

Deleted: .

Deleted: In contrast,

Deleted: responded much more

Deleted: than in treatment D

Deleted: tended to

Deleted: HPLC data

Deleted: take place

Deleted: in

Deleted: during this experiment

Deleted: sampling time

Deleted: at

Deleted: Both under ambient and future conditions, a

Deleted: appeared even

Deleted: observed

Deleted: ambient

Deleted: levels

Deleted: evaluate with no clear effects of dust addition or

Deleted: pH/temperature conditions and with a

Deleted: decrease

effects of treatments were detected. At station FAST, although the sample size was too low to statistically test for differences, higher total abundances of meso-zooplankton species were observed in the dust-amended tanks with no differences between ambient and future conditions of temperature and pH. However, differences in abundance were visible between these two treatments for specific groups, with respectively higher abundance of Harosa and lower abundance of Crustacea (other than copepods) and Mollusca in warmed and acidified tanks.

4. Discussion

4.1. Initial conditions

During this study, the mixed layer depth (MLD) was somewhat shallower at TYR (20 m) than at ION and FAST (~ 10 and ~15 m, respectively) at the time of the sampling (Van Wambeke et al., 2020a). Such shallow MLDs are characteristic of the stratified and oligotrophic conditions encountered in the western Mediterranean basin in late spring/early summer (D'Ortenzio et al., 2005). Although direct measurements of NO_x and DIP concentrations using nanomolar techniques (as performed in our study) are scarce in the Mediterranean Sea, the low levels measured during the cruise are in agreement with DIP values reported for the three basins (Djaoudi et al., 2018) and with NO_x and DIP concentrations measured in coastal waters of Corsica in late spring/early summer (Louis et al., 2017b; Pulido-Villena et al., 2014; Ridame et al., 2014). NO_x:DIP molar ratios in surface waters were well below the Redfield ratio (16:1) and are also consistent previous studies. The low NO_x:DIP ratios and nutrient concentrations suggest that communities found at the three stations experienced N and P co-limitation at the start of the experiments, as previously shown by Tanaka et al. (2011). Nutrient enrichment experiments confirmed that, at the three sites, heterotrophic bacteria were mainly N-P co-limited (Van Wambeke et al., 2020b). In contrast to N and P, dissolved Fe in surface seawater, ranged from 1.5 nmol L^{-1} at TYR to 2.5 nmol L^{-1} at ION (Roy-Barman et al., 2021) and were unlikely limiting for biological activity as previously shown in the Mediterranean Sea under stratified conditions (Bonnet et al., 2005; Ridame et al., 2014).

The low total chlorophyll *a* concentrations in surface waters were typical for the Western and Central Mediterranean Sea in late spring/early summer, as estimated from remote sensing (Bosc et al., 2004), and from *in situ* measurements (Manca et al., 2004). While large species (i.e. diatoms, dinoflagellates) represented only ~10% of the total chlorophyll *a* biomass, the

Deleted: Over the transect,
Deleted: occupied the first 20 m. It
Deleted: as compared to
Deleted: mixed layer depth, MLD of
Deleted: vs
Deleted: is well representative
Deleted: Overall, the three experiments were conducted with surface seawater collected during oligotrophic conditions typical of the open Mediterranean Sea at this period of the year (late spring).
Deleted: studied
Deleted: Furthermore, at all three stations,
Deleted: the tested
Deleted: with ratios found in these
Deleted: ly
Deleted: cited
Deleted: Both
Deleted: low
Deleted: A side n
Deleted: initial concentrations of
Deleted: the sampled
Deleted: i
Deleted: ng
Deleted: 0
Formatted: English (US)
Deleted: ,
Deleted: L
Deleted: the tested
Deleted: representative of surface concentrations reported
Deleted: both from
Deleted: images
Deleted: provided in a database from Manca et al.
Deleted: of the tested waters

composition of the smaller size phytoplankton communities differed substantially, with autotrophic nano-eukaryotes dominating at stations TYR and ION and a larger contribution from autotrophic pico-eukaryotes and Cyanobacteria at station FAST. Due to their low competitiveness under nutrient limitation, the small contribution of large phytoplankton cells at the start of the experiment is a fingerprint of LNLC areas in general, and of surface Mediterranean waters in late spring and summer (Siokou-Frangou et al., 2010).

Biomass of both heterotrophic nanoflagellates and prokaryotes followed a west to east gradient (FAST > TYR > ION), with high relative contribution by heterotrophs at stations TYR and FAST (60% of biomass) while at ION autotrophs contributed 60% to plankton biomass. Accordingly, net community production (NCP) rates (Gazeau et al., 2021) showed an initial community close to metabolic balance (mean ± SE: -0.06 ± 0.09 µmol O_2 L^{-1} d^{-1}) at ION and highest community respiration rates and consequently lowest NCP rates at station TYR (-1.9 µmol O_2 L^{-1} d^{-1}) suggesting that the autotrophic plankton community was not very active and relied on regenerated nutrients, as shown by the high level of NH_4^+ at the start of the experiment at TYR. In contrast, although slightly heterotrophic (Gazeau et al., 2021) and limited by the low amount of nutrients, the community at FAST showed by the highest levels of ^{14}C production and heterotrophic prokaryote production (Gazeau et al., 2021) as well as N_2 fixation (Céline Ridame, unpublished results). Altogether, the heterotrophic signature of the three investigated stations, although closer to metabolic balance at ION, reflected typical biogeochemical conditions in the Mediterranean Sea during late spring to early summer (Regaudie-de-Gioux et al., 2009).

4.2. Critical assessment of the experimental system and methodology

The experimental tanks used in this study have been successfully validated in previous studies designed to investigate the inputs of macro- and micro-nutrients (e.g. NO_x, DIP, DFe)

Deleted: . Indeed,

Deleted: communities were clearly dominated by

Deleted: was observed

Deleted: As b

Deleted: the ratio of autotrophic vs

Deleted: heterotrophic

Deleted: biomass appeared clearly in favor of the heterotrophic compartment

Deleted: ratio of 0.6

Deleted: a value above 1 was estimated

Deleted: (ratio of 1.3)

Deleted: This is coherent

Deleted: with the highest

Deleted: being reported at this station by Gazeau et al.

Deleted: ing

Deleted: that the

Deleted: at the start of this experiment was very

Deleted: .

Deleted: The

Deleted: were measured

Deleted: further

Deleted: ying

Deleted: est

Deleted: measured

Deleted: this

Deleted: of the tested waters

Deleted: was the most active as

Deleted: n

and the export of organic matter, under close-to-abiotic conditions (natural seawater filtered onto 0.2 µm) following simulated wet dust events using the same analog as used in our study (Bressac and Guieu, 2013; Louis et al., 2017a, 2018). Louis et al. (2017a, 2018) further investigated these impacts under lowered pH conditions resulting in a rapid increase of pH levels in the acidified filtered seawater due to CO_2 outgassing (from ~7.4 to ~7.7 in six days). In the present study, our experimental system further allowed to control atmospheric pCO_2 in addition to light and temperature (i.e. climate reactors). Thereby, this allowed to significantly reduce CO_2 outgassing and maintain pH levels close to their targets. The regulation of atmospheric CO_2 was, however, consistently more efficient in tank G2 compared to G1 (Fig. 5), resulting in a small discrepancy in terms of pH (highest difference of 0.04 pH units between the two G tanks at FAST), possibly due to a potential leak or a longer flushing time above tank G1. Nevertheless, as no systematic differences in nutrient dynamics and biological response were observed between the two tanks, these small differences in pH had no detectable effect on the obtained results.

The lids above tanks, equipped with LEDs in order to reproduce sunlight intensity and spectrum, were used for the first time during these experiments. While simulated intensities were close to estimates for the Northwestern Mediterranean Sea at 5 m depth in June (~1100 µmol photons m^{-2} s^{-1}; Bernard Gentili, personal communication, 2017) and fairly consistent between duplicates under control and dust-amended conditions, largest differences were also observed between tanks G1 and G2. These discrepancies could result from small differences in PAR sensors calibration and/or of different turbidity related to the amount of particles remaining in the tanks. As for pH, replication in terms of macronutrient dynamics and biological response appeared satisfactory (except at station TYR; see below).

Continuous measurements in the tanks showed that temperature was not spatially homogeneous, leading to significant differences among replicates. This was more pronounced for warmed tanks (treatment G) with a maximum average difference over the experimental

Deleted: seawater filtration

Deleted: , although no control of atmospheric pCO_2 was performed …

Deleted: Since those above-mentioned studies, in order to avoid this,

Deleted: we improved

Deleted: to

Deleted: mimicking future conditions by

Deleted: ling

Deleted: T

Deleted: experimental

Deleted: Still, as illustrated in Fig. 5, t

Deleted: in terms of

Deleted:

Deleted: se

Deleted: we believe that

Deleted: terms of regulated

Deleted: consequences

Deleted: r

Deleted: the two warmed and acidified

Deleted: The reasons of t

Deleted: terms of light intensity regulation between lids, of

Deleted: discussed above

Deleted: for this treatment

Deleted: , and we believe these technical issues had no significant impacts on our results.

Deleted: especially the case

Deleted: for which

Deleted: al

period of 0.7 °C during the FAST experiment. As for pH and light, these discrepancies did not systematically lead to observable differences in the investigated stocks and processes between duplicates (except at TYR, see below).

The necessity to carry out the incubations in a clean container limited our possibility to set up additional replicates for the three treatments. As described above, differences between duplicates were, for the vast majority of studied variables and processes, lower than differences between treatments and appear robust considering the difficulty to incubate plankton communities for which slight differences in initial composition can translate into important differences in dynamics (Eggers et al., 2014). Nevertheless, important discrepancies were detected for autotrophic stocks (in particular Synechococcus) as well as HNF and processes (Gazeau et al., 2021) for the warmed and acidified treatment (tanks G1 and G2) at station TYR. The reasons behind these differences are most likely due to the grazing impact of heterotrophic nano-flagellates on prokaryotic picoplankton (Sherr and Sherr, 1994) in tank G1 where HNF abundance sharply increased during the experiment. Overall, while the methodology used in this study allowed to successfully evaluate the impacts of dust addition under both present and future environmental conditions at two out of three tested waters, the discrepancies at station TYR prevent us from drawing any strong conclusion on the effect of dust addition on the dynamics of the community under future environmental conditions at that station.

4.3. Impact of dust addition under present environmental conditions

During all experiments, the observed increases in NO_x and DIP few hours after dust addition under present environmental conditions were similar to the enrichment obtained during the DUNE experiments at the surface of the mesocosms (~ 50 m^3) after the simulation of a wet dust deposition using the same dust analog and the same simulated flux (Pulido-Villena et al.,

Deleted: was observed

Deleted: the other controlled parameters discussed above

Deleted: relatively low number of experimental units that could be installed inside an embarkable

Deleted: restrained

Deleted: consider

Deleted: more than two replicates per

Deleted: Fortunately, as already said

Deleted: acceptable

Deleted: their

Deleted: very

Deleted: we have to note that

Deleted: regarding

Deleted: tanks of

Deleted: not fully understood but we strongly suspect that

Deleted:

Deleted: , feeding mainly

Deleted: ,

Deleted: exerted a strong top-down control on this group

Deleted: in which

Deleted: All in all

Deleted: se

Deleted: the three

Deleted: rather

Deleted: levels

2014; Ridame et al., 2014). The intensity of the simulated wet deposition event (i.e. 10 g m^{-2}) represents a high but realistic scenario, as several studies reported even higher short wet deposition events in this area of the Mediterranean Sea (Bonnet and Guieu, 2006; Loÿe-Pilot and Martin, 1996; Ternon et al., 2010). Furthermore, based on previous studies reporting the mixing between dust and polluted air masses during the atmospheric transport of dust particles (e.g. Falkovich et al., 2001; Putaud et al., 2004), we used an evapo-condensed dust analog that mimics the processes taking place in the atmosphere prior to deposition, essentially the adsorption of inorganic and organic soluble species (e.g. sulfate and nitrate; see Guieu et al., 2010a, for further details). The imposed evapo-condensation processes are responsible for the large nitrate releasing capacity of the dust particles used in our study. As a consequence, the addition of new nutrients from dust in our study and during the P and R DUNE experiments were much higher, especially for NO_x, than those observed by Pitta et al. (2017, and references therein) and Ridame et al. (2014) following the simulation of a dry Saharan dust deposition event. This confirms that wet dust deposition is a more efficient source of bioavailable nutrients than dry dust deposition.

Although NO_x and DIP increases after dust addition were similar in all experiments, the subsequent dynamics of these elements and the impacts on plankton community composition and functioning were drastically different. While NO_x levels decreased moderately over the course of our experiments due to biological uptake, more abrupt decreases were observed for DIP released by dust, reaching values close to the ones observed in the controls, except at station FAST where concentrations were still above ambient levels at the end of the experiment.

Previous experiments on the effect of dust addition in the Mediterranean Sea showed significant increases in chlorophyll *a* concentrations (mean ~90% increase; Guieu and Ridame, 2020). Interestingly, no stimulation of autotrophic biomass and primary production rates (Gazeau et al., 2021) was observed in dust-amended tanks under present conditions at station TYR. To the best of our knowledge, this is the first experimental evidence of a complete absence of response

Deleted: this

Deleted: chose to

Deleted: compared to

Deleted: rather

Deleted: during our three

Deleted: Regarding biological stocks, most

Deleted: reporting

from an autotrophic community following dust wet deposition. The absence of response from autotrophic stocks could be due to a tight top-down control by grazers hiding potential responses from the autotrophic community (Lekunberri et al., 2010; Marañón et al., 2010) and/or a competition for nutrients with heterotrophic prokaryotes (Marañón et al., 2010). Feliú et al. (2020) have shown that the mesozooplankton assemblage at TYR was clearly impacted by a dust event that took place nine days before sampling at that station as evidenced from particulate inventory of lithogenic proxies (Al, Fe) in the water column (Bressac et al., 2021), likely stimulating phytoplankton growth and consequently increased the abundance of herbivorous grazers (copepods) and attracted carnivorous species well before the start of the experiment. Heterotrophic bacteria are also limited by inorganic nutrients, mainly DIP, in oligotrophic systems (Obernosterer et al., 2003; Van Wambeke et al., 2001). Recent studies have shown significant increases in heterotrophic bacterial abundance, respiration and/or production following dust deposition (and nutrient enrichment) in these areas (Lekunberri et al., 2010; Pitta et al., 2017; Pulido-Villena et al., 2008; Romero et al., 2011). Heterotrophs appear to be more stimulated by dust pulses than autotrophic plankton with increasing degree of oligotrophy, modulated by the competition for nutrients between phytoplankton and bacteria (Marañón et al., 2010). This response was reflected at station TYR, with heterotrophic prokaryotes reacting quickly and strongly to nutrient addition both in terms of abundances and production rates (Gazeau et al., 2021). These two aforementioned hypotheses are not mutually exclusive, and the quick response of heterotrophic prokaryotes to dust addition is coherent with the net heterotrophy at this station (see 4.1) due to increases in community respiration and decreases in net community production rates in dust-amended as compared to control tanks (Gazeau et al., 2021). Hence, dust addition to surface waters strongly dominated by heterotrophs leads to a reduction of the capacity of these communities to export organic matter and sequester atmospheric CO_2.

Deleted: from

Deleted: tive resources

Deleted: Regarding the first hypothesis,

Deleted: (Bressac et al., in preparation)

Deleted: . This dust deposition likely

Deleted: ed

Deleted: With respect to the second hypothesis, it is well known that not only phytoplankton but also h

Deleted: Indeed, many r

Deleted: .

Formatted: French

Deleted: Most of the time, h

Deleted: ic

Deleted: processes

Deleted: compared to

Deleted: processes

Deleted: the dominant response being

Deleted: is clearly what was observed at this

Deleted:

Deleted: strongest

Deleted: of the tested waters

Deleted: . The strong stimulation of heterotrophic prokaryotes and the absence of detectable effects on the autotrophic compartment drove the community towards an even stronger net heterotrophic state as illustrated by the decrease in the autotrophic to heterotrophic biomass ratio following dust addition (data not shown). This was further shown by…

Deleted: and suggest that

Deleted: waters

In contrast to the dynamics of the experiment at TYR, stimulation of primary producers was observed at stations ION and FAST under present conditions with overall higher impact than previous studies compiled by Guieu and Ridame (2020). The largest increase in chlorophyll *a* concentrations at station FAST is coherent with NO_x decreases observed at this station. Interestingly, at FAST, DIP concentrations were still above ambient conditions at the end of the experiment. Maximum primary production rates (^{14}C-incorporation) at the end of the experiment suggest strong DIP recycling and the dominance of regenerated production towards the end of the experiment (Gazeau et al., 2021). Although, in some cases, *Synechococcus* appeared stimulated by dust addition (Herut et al., 2005; Lagaria et al., 2017; Paytan et al., 2009), Guieu et al. (2014b) showed that, based on the analysis of several aerosols addition studies, this group had generally weak responses to aerosol addition in contrast to nano- and micro-phytoplankton, suggesting that aerosol deposition may lead to an increase in larger phytoplankton. Yet, at stations ION and FAST, the increase in *Synechococcus* abundance in dust-amended tanks was the highest relative to those of pico- and nano-eukaryotes. In particular, at station ION, no clear response to nutrient enrichment was observed for nano-eukaryotes throughout the experiment. However, it must be stressed that our experiments were of a relatively short period (3 to 4 days). The sharp increase in Fucoxanthin paralleled by a decrease in silica, at the end of the experiment at station FAST where DIP limitation was not yet apparent, suggests a delayed response of diatoms as compared to smaller taxa. The sharp decline in nano-eukaryote abundances in dust-amended tanks at the end of the FAST experiment, further suggests that this group reacted quickly to nutrient enrichment and was progressively grazed and/or outcompeted by larger phytoplankton species.

While, all groups of primary producers benefited from nutrient enrichment at FAST, the increases in heterotrophic prokaryote abundances were moderate, leading to an increase of net community production rates throughout the experiment, reaching positive levels and a

Deleted: what was observed
Deleted: fertilization
Deleted: relative changes much
Deleted: from
Deleted: the largest
Deleted: in our study, which occurred
Deleted: following dust addition at this station
Deleted: , autotrophic production did not lead to DIP exhaustion throughout the experiment as
Deleted: Maximal
Deleted: at this station
Deleted: a
Deleted: size class
Deleted: This was especially true
Deleted: where
Deleted: performed over
Deleted: , and t
Deleted: tes
Deleted: groups (i.e. autotrophic prokaryotes, pico- and nano-eukaryotes). Although this was not observed based on pigment analyses,
Deleted: the
Deleted: ,
Deleted: reacting
Deleted: In contrast to what was observed at TYR, at station FAST, the competition for nutrients between autotrophs and heterotrophs was clearly in favor of autotrophs with a clear increase in the ratio between autotrophic and heterotrophic biomass reaching values of up to 4 (data not shown).
Deleted: as discussed above,
Deleted: this station
Deleted: rather limited following dust deposition
Deleted: is
Deleted: to reach

autotroph:heterotroph ratio of 4, while control tanks remained below metabolic balance (Gazeau et al., 2021). At station ION, the situation was intermediate with a similar enhancement of both autotrophic and heterotrophic stocks and no clear changes in the ratio between autotrophic and heterotrophic biomass (data not shown), although the system evolved towards net autotrophy at the end of the experiment in dust -amended tanks under present environmental conditions (Gazeau et al., 2021).

Transfer of newly produced organic matter to higher trophic levels in the different treatments was assessed through the quantification of meso-zooplankton abundance at the end of each experiment. Altogether it is not surprising that an increase in meso-zooplankton abundances was only detected at station FAST where the strongest enhancement of primary production was observed. Such an increase in meso-zooplankton abundance in the dust-amended as compared to control treatment was observed during land-based mesocosm experiments in the Eastern Mediterranean Sea (Pitta et al., 2017).

Finally, although no clear effects of dust deposition under present conditions were detectable on autotrophic prokaryotes at station TYR, the strongest increase in N_2 fixation rates was recorded at this station (Céline Ridame, unpublished results). However, the potential impact of this process on NO_x concentration is negligible compared to the very large stock of NO_x present in the dust-amended tanks, as less than 1 nmol L^{-1} d^{-1} of NO_x was produced through N_2 fixation (Céline Ridame, unpublished results).

4.4. Impact of dust addition under future environmental conditions

Few studies have investigated the release and fate of nutrients from atmospheric deposition under climate conditions as expected for the end of the century, and, to the best of our

Deleted: somewhat

Deleted: appeared in favor of

Deleted: evaluated

Deleted: Although we are fully aware that such an approach is certainly criticizable considering the low incubation times (3 to 4 days), it may still be representative of lowered mortality or faster growth.

Deleted: does not appear as a

Deleted: e

Deleted: highly

Deleted: can be produced by this process

Formatted: Subscript

Deleted: Very f

Deleted: past

Deleted: particles

knowledge, our study represents the first attempt to test for the combined effect of ocean warming and acidification on these processes. The study by Louis et al. (2018), carried out with filtered (0.2 µm mesh size) natural seawater using the same dust analog and flux as in the present study showed that even an extreme ocean acidification scenario (~ -0.6 pH units) does not impact the bioavailability of macro- and micro-nutrients (NO_x, DIP and DFe) in the oligotrophic Northwestern Mediterranean Sea. Similar results were found by Mélançon et al. (2016) in high-nutrient low-chlorophyll (HNLC) waters of the Northeastern Pacific, under a moderate ocean acidification scenario (-0.2 pH units). As no differences were observed for NO_x and DIP concentrations within a few hours following dust addition under present and future environmental conditions, our results agree with these previous findings and further highlights the absence of direct effect of ocean warming (+3 °C) on the release of nutrients from atmospheric particles.

In contrast, different nutrient consumption dynamics were observed between ambient and warmed/acidified tanks. No impacts of warming and acidification could be observed for NO_x at stations TYR and ION due to low net uptake rates compared to the large increase following dust addition. In contrast, at the most productive station FAST, as a consequence of strongly enhanced biological stocks (see thereafter) and metabolic rates (Gazeau et al., 2021), larger NO_x consumption rates were shown under future environmental conditions.

The differences in DIP dynamics between the two dust-amended treatments were more complex to interpret. A clear feature of our experiments is that, in contrast to present day pH and temperature conditions, all the stock of DIP released from dust was consumed at the end of the three experiments under future conditions. The rate of decrease differed depending on the station. While DIP dynamics were quite similar between tanks maintained under present and future environmental conditions at ION, warming and acidification induced a faster decrease of DIP at TYR and FAST, with a full consumption of the released DIP within 24 h. An interesting

Formatted: English (US)
Formatted: Font: (Default) Times New Roman, 12 pt, English (US)
Field Code Changed
Formatted: Font: (Default) Times New Roman, English (US)
Formatted: English (US)
Deleted: have already shown from an experiment performed under close-to-abiotic conditions (seawater filtration onto 0.2 µm) …
Deleted: from dust addition for surface phytoplankton communities …
Deleted: , using the same dust analog and simulated flux as used during our experiments
Deleted: presented
Deleted: regarding the release of DFe from dust
Deleted: following
Deleted: mild
Deleted: of
Deleted: , following these similar nutrient releases
Deleted: These differences were substantially dependent on the considered nutrient and investigated station.
Deleted: Regarding NO_x, n
Formatted: Subscript
Deleted: decreasing
Deleted: .
Deleted: depending on the investigated station
Deleted: , suggesting a much faster consumption by autotrophs and heterotrophic prokaryotes
Deleted: That being said, t
Deleted: under future environmental conditions

outcome at station TYR was that, despite the important discrepancies observed for autotrophic stocks and metabolic rates between the duplicates G1 and G2 (see section 4.2), a similar dynamics was observed for DIP concentrations in these tanks. As heterotrophic prokaryote biomass and production rates (Gazeau et al., 2021) did not differ between these duplicate tanks, this further highlights the clear dominance of heterotrophic processes at this station, a dominance which was exacerbated by dust addition under future environmental conditions, leading to an even stronger heterotrophic state at the end of this experiment (Gazeau et al., 2021).

At station ION, large impacts of warming and acidification were found with twice the chlorophyll *a* concentrations than in the dust amended D tanks. At this station, all autotrophic groups increased with ocean acidification and warming. *Synechococcus* and to a lesser extent pico-eukaryotes showed the strongest response. Yet these differences in abundance did not lead to detectable changes in the composition of the autotrophic assemblage, with nano-eukaryote largely dominating carbon biomass at the end of this experiment (62% in treatment G vs. 64% in treatment D). Although the ratio between autotrophic and heterotrophic biomass appeared positively impacted under future environmental conditions, reaching values of up to 2 at the end of the experiment, warming and acidification led to a decrease in net community production (Gazeau et al., 2021) suggesting that in the coming decades the capacity of surface seawater to sequester anthropogenic CO_2 will be lowered.

Similarly, at FAST, all phytoplankton groups were impacted positively by warming and acidification with the strongest changes detected for *Synechococcus* as compared to present environmental conditions. However, in contrast to station ION, all groups reached maximal abundances (and carbon biomass) after 3 days of incubations, thereafter drastically decreasing most likely as a consequence of DIP limitation (see above). It must be stressed that this pattern could not be observed from pigments as no samples were taken for these analyses after 3 days of incubation. Also, in contrast to station ION, the abundance of heterotrophic prokaryotes in the

Deleted: very

Deleted: have been observed

Deleted: , especially for primary producers, as shown by almost…doubled
doubled

Deleted: doubled

Deleted: as compared to

Deleted: (D)

Deleted: benefited from

Deleted: appeared as the most impacted ones

Deleted: of sensitivity among autotrophs

Deleted: as compared to ambient conditions

Deleted: still a large dominance of

Deleted: Interestingly, a

Deleted: positively

Deleted: is

Deleted: (data not shown)

Deleted: through

Deleted: dynamics

Deleted: sampling was performed

warmer and acidified treatment reached a maximum after 2 days of incubations and then decreased rapidly to reach levels observed in the control treatment. This suggests that heterotrophic prokaryotes were the first to suffer from DIP limitation and further highlights the dominance of autotrophs in terms of nutrient consumption at this station. Although the ratio between autotrophic and heterotrophic biomass increased under future environmental conditions at ION, Gazeau et al. (2021) reported on a decrease in net community production rates in this treatment as compared to ambient environmental conditions, suggesting that, in the future, nutrient release from dust will lead to a lesser sequestration capacity of surface waters for atmospheric CO_2.

The positive effects of warming and acidification on the abundance of mostly small (< 20 µm) phytoplankton taxa, as observed at ION and FAST, are in line with previously published studies. Although the effect of ocean acidification on small autotrophic species shows a wide range (e.g. Dutkiewicz et al., 2015), there is increasing evidence that small phytoplankton species will be favored in a warmer ocean (e.g. Chen et al., 2014; Daufresne et al., 2009; Morán et al., 2010). Our experimental protocol was not conceived to discriminate temperature from pH effects, however results concur with those of Maugendre et al. (2015) which further suggested temperature over elevated CO_2 as the main driver of increased picophytoplankton abundance in the Mediterranean Sea.

These enhanced fertilizing effects on primary producers at ION and FAST, under future as compared to present environmental conditions, did not seem to reach higher trophic levels as no clear differences in meso-zooplankton abundances were observed between ambient and warmed/acidified tanks at the end of the experiments. The duration of our experiments was too short to carefully assess the proportion of newly formed organic matter consumed by meso-zooplankton species and its effect on their biomass, yet group-specific variations were observed.

Deleted: strongly

Deleted: the

Deleted: compartment

Deleted: was

Deleted: the

Deleted: ic

Deleted: compartment

Deleted: As observed at station ION, a

Formatted: Indent: First line: 1.27 cm

Deleted: se

Deleted: cells

Deleted: , especially for small species

Deleted: Indeed, a

Deleted: very contrasted results have been shown on

Deleted: As mentioned earlier, o

Deleted: We fully acknowledge that t

Deleted: certainly

Deleted: abundances

Finally, Gazeau et al. (2021) did not observe an additional impact of future environmental conditions on the export of organic matter after dust addition.

Deleted: Similarly

5. Conclusion

These experiments conducted during the PEACETIME cruise represent the first attempt to investigate the impacts of atmospheric deposition on surface plankton communities both under present and future environmental conditions. Despite few experimental issues that are discussed, the three experiments provided new insights on these potential impacts in the open Mediterranean Sea. Stark differences in the response to dust deposition were observed between the three investigated stations in the Tyrrhenian Sea, Ionian Sea and in the Algerian basin. Given that the initial conditions at the three stations were very similar in terms of nutrient and chlorophyll concentrations, these differences seem to be rather a consequence of the initial metabolic states of the community (autotrophy vs. heterotrophy). In all three cases, nutrient addition from dust deposition did not strongly modify but rather exacerbated this initial state. Relative changes in main parameters presented in this manuscript and processes presented in Gazeau et al. (2021) as a consequence of dust addition under present and future environmental conditions are shown in Fig. 10, and compared to the compilation of published data for the Mediterranean Sea from Guieu and Ridame (2020). At station TYR, under conditions of a clear dominance of heterotrophs on the use of resources and potentially a higher top-down control from grazers, dust addition drove the community into an even more heterotrophic state with no detectable effect on primary producers. At station ION, where the community was initially closer to metabolic balance, both heterotrophic and autotrophic compartments benefited from dust derived nutrients. At FAST, the station with the highest initial autotrophic production, addition of nutrients led to an increase in both compartments but heterotrophic prokaryotes became quickly P-limited and overall larger effects were observed for phytoplankton. Ocean acidification and warming did not have any detectable impact on the release of nutrients from atmospheric particles. Furthermore, these external drivers did not drastically modify the composition of the autotrophic assemblage

Deleted: that are discussed

Formatted: Font: (Default) Times New Roman, 12 pt, Font colour: Auto, English (US)

Deleted: Interestingly, the effect of dust deposition was highly different

Deleted: As the

Deleted: in the sampled surface seawater

Deleted: availability

Deleted:

Deleted: content

Deleted: rather

Deleted: most active

Deleted: in terms of

Deleted: boosted

with all groups benefiting from warmer and acidified conditions. However, although for two out of the three stations investigated, larger increases were observed for autotrophic as compared to heterotrophic stocks under future environmental conditions, a stronger impact of warming and acidification on mineralization processes (Gazeau et al., 2021) suggests that, in the future, the plankton communities of Mediterranean surface waters will have a decreased capacity to sequester atmospheric CO_2 following the deposition of atmospheric particles.

Data availability

All data and metadata will be made available at the French INSU/CNRS LEFE CYBER database (scientific coordinator: Hervé Claustre; data manager, webmaster: Catherine Schmechtig). INSU/CNRS LEFE CYBER (2020)

Author contributions

FG and CG designed and supervised the study. FG, CG, CR and KD sampled seawater from the experimental tanks during the experiments. JMG and GDL participated in the technical preparation of the experimental system and all authors participated in sample analyses. FG, CR and CG wrote the paper with contributions from all authors.

Financial support

This study is a contribution to the PEACETIME project (http://peacetime-project.org), a joint initiative of the MERMEX and ChArMEx components supported by CNRS-INSU, IFREMER, CEA, and Météo-France as part of the programme MISTRALS coordinated by INSU. PEACETIME is a contribution to SOLAS and IMBER international programme. The project was endorsed as a process study by GEOTRACES. PEACETIME cruise (https://doi.org/10.17600/17000300). The project leading to this publication has also received funding from the European FEDER Fund under project 1166-39417.

Acknowledgments

The authors thank the captain and the crew of the RV Pourquoi Pas ? for their professionalism and their work at sea. We thank Julia Uitz, Céline Dimier and the SAPIGH HPLC analytical service at Institut de la Mer de Villefranche (IMEV) for sampling and analysis of phytoplankton pigments, John Dolan for microscopic countings as well as Lynne Macarez and the PIQv-

1576 platform of EMBRC-France, a national Research Infrastructure supported by ANR, under the
1577 reference ANR-10-INSB-02, for mesozooplankton analyses.

References

Aminot, A. and Kérouel, R.: Dosage automatique des nutriments dans les eaux marines : méthodes en flux continu, Editions Ifremer, méthodes d'analyse en milieu marin, 188 pp., 2007.

Behrenfeld, M. J., O'Malley, R. T., Siegel, D. A., McClain, C. R., Sarmiento, J. L., Feldman, G. C., Milligan, A. J., Falkowski, P. G., Letelier, R. M., and Boss, E. S.: Climate-driven trends in contemporary ocean productivity, Nature, 444, 752–755, 2006.

Bergametti, Gi., Dutot, A.-L., Buat-Ménard, P., Losno, R., and Remoudaki, E.: Seasonal variability of the elemental composition of atmospheric aerosol particles over the Northwestern Mediterranean, 41, 353–361, https://doi.org/10.3402/tellusb.v41i3.15092, 1989.

Bonnet, S. and Guieu, C.: Atmospheric forcing on the annual iron cycle in the western Mediterranean Sea: A 1-year survey, 111, https://doi.org/10.1029/2005JC003213, 2006.

Bonnet, S., Guieu, C., Chiaverini, J., Ras, J., and Stock, A.: Effect of atmospheric nutrients on the autotrophic communities in a low nutrient, low chlorophyll system, 50, 1810–1819, https://doi.org/10.4319/lo.2005.50.6.1810, 2005.

Børsheim, K. Y. and Bratbak, G.: Cell volume to cell carbon conversion factors for a bacterivorous Monas sp. enriched from seawater, 36, 171–175, 1987.

Bosc, E., Bricaud, A., and Antoine, D.: Seasonal and interannual variability in algal biomass and primary production in the Mediterranean Sea, as derived from 4 years of SeaWiFS observations, 18, https://doi.org/10.1029/2003GB002034, 2004.

Bressac, M. and Guieu, C.: Post-depositional processes: What really happens to new atmospheric iron in the ocean's surface?, 27, 859–870, https://doi.org/10.1002/gbc.20076, 2013.

Bressac, M., Guieu, C., Doxaran, D., Bourrin, F., Desboeufs, K., Leblond, N., and Ridame, C.: Quantification of the lithogenic carbon pump following a simulated dust-deposition event in large mesocosms, 11, 1007–1020, https://doi.org/10.5194/bg-11-1007-2014, 2014.

Formatted: Indent: Left: 0 cm, Hanging: 1 cm, Line spacing: Double

Formatted: French

Bressac, M., Wagener, T., Leblond, N., Tovar-Sánchez, A., Ridame, C., Albani, S., Guasco, S., Dufour, A., Jacquet, S., Dulac, F., Desboeufs, K., and Guieu, C.: Subsurface iron accumulation and rapid aluminium removal in the Mediterranean following African dust deposition, Biogeosciences Discussions, 1–29, https://doi.org/10.5194/bg-2021-87, 2021.

Chen, B., Liu, H., Huang, B., and Wang, J.: Temperature effects on the growth rate of marine picoplankton, 505, 37–47, https://doi.org/10.3354/meps10773, 2014.

Christaki, U., Courties, C., Massana, R., Catala, P., Lebaron, P., Gasol, J. M., and Zubkov, M. V.: Optimized routine flow cytometric enumeration of heterotrophic flagellates using SYBR Green I, 9, 329–339, https://doi.org/10.4319/lom.2011.9.329, 2011.

Daufresne, M., Lengfellner, K., and Sommer, U.: Global warming benefits the small in aquatic ecosystems, PNAS, 106, 12788–12793, https://doi.org/10.1073/pnas.0902080106, 2009.

Desboeufs, K., Leblond, N., Wagener, T., Bon Nguyen, E., and Guieu, C.: Chemical fate and settling of mineral dust in surface seawater after atmospheric deposition observed from dust seeding experiments in large mesocosms, 11, 5581–5594, https://doi.org/10.5194/bg-11-5581-2014, 2014.

Desboeufs, K., Bon Nguyen, E., Chevaillier, S., Triquet, S., and Dulac, F.: Fluxes and sources of nutrient and trace metal atmospheric deposition in the Northwestern Mediterranean, 18, 14477–14492, https://doi.org/10.5194/acp-18-14477-2018, 2018.

Dickson, A. G., Sabine, C. L., and Christian, J. R.: Guide to best practices for ocean CO2 measurements, PICES, Sydney, 191 pp., 2007.

Dinasquet, J., Bigeard, E., Gazeau, F., Azam, F., Guieu, C., Marañón, E., Ridame, C., Van Wambeke, F., Obernosterer, I., and Baudoux, A.-C.: Impact of dust addition on the microbial food web under present and future conditions of pH and temperature, Biogeosciences Discussions, 1–48, https://doi.org/10.5194/bg-2021-143, 2021.

Djaoudi, K., Van Wambeke, F., Coppola, L., D'Ortenzio, F., Helias-Nunige, S., Raimbault, P., Taillandier, V., Testor, P., Wagener, T., and Pulido-Villena, E.: Sensitive Determination of

Formatted: Font: (Default) Times New Roman

Deleted: Bressac, M., Wagener, T., Tovar-Sanchez, A., Ridame, C., Albani, S., Fu, F., Desboeufs, K., and Guieu, C.: Residence time of dissolved and particulate trace elements in the surface Mediterranean Sea (Peacetime cruise), in preparation.¶

Formatted: Font: (Default) Times New Roman

Formatted: Font: (Default) Times New Roman

Formatted

the Dissolved Phosphate Pool for an Improved Resolution of Its Vertical Variability in the Surface Layer: New Views in the P-Depleted Mediterranean Sea, Front. Mar. Sci., 5, https://doi.org/10.3389/fmars.2018.00234, 2018.

D'Ortenzio, F., Iudicone, D., Montegut, C. de B., Testor, P., Antoine, D., Marullo, S., Santoleri, R., and Madec, G.: Seasonal variability of the mixed layer depth in the Mediterranean Sea as derived from in situ profiles, 32, https://doi.org/10.1029/2005GL022463, 2005.

Duce, R. A., Liss, P. S., Merrill, J. T., Atlas, E. L., Buat-Menard, P., Hicks, B. B., Miller, J. M., Prospero, J. M., Arimoto, R., Church, T. M., Ellis, W., Galloway, J. N., Hansen, L., Jickells, T. D., Knap, A. H., Reinhardt, K. H., Schneider, B., Soudine, A., Tokos, J. J., Tsunogai, S., Wollast, R., and Zhou, M.: The atmospheric input of trace species to the world ocean, Global Biogeochemical Cycles, 5, 193–259, https://doi.org/10.1029/91GB01778, 1991.

Dutkiewicz, S., Morris, J. J., Follows, M. J., Scott, J., Levitan, O., Dyhrman, S. T., and Berman-Frank, I.: Impact of ocean acidification on the structure of future phytoplankton communities, 5, 1002–1006, https://doi.org/10.1038/nclimate2722, 2015.

Emerson, S., Quay, P., Karl, D., Winn, C., Tupas, L., and Landry, M.: Experimental determination of the organic carbon flux from open-ocean surface waters, 389, 951–954, https://doi.org/10.1038/40111, 1997.

Falkovich, A. H., Ganor, E., Levin, Z., Formenti, P., and Rudich, Y.: Chemical and mineralogical analysis of individual mineral dust particles, 106, 18029–18036, https://doi.org/10.1029/2000JD900430, 2001.

Feliú, G., Pagano, M., Hidalgo, P., and Carlotti, F.: Structure and function of epipelagic mesozooplankton and their response to dust deposition events during the spring PEACETIME cruise in the Mediterranean Sea, 17, 5417–5441, https://doi.org/10.5194/bg-17-5417-2020, 2020.

Gazeau, F., Van Wambeke, F., Marañón, E., Pérez-Lorenzo, M., Alliouane, S., Stolpe, C., Blasco, T., Leblond, N., Zäncker, B., Engel, A., Marie, B., Dinasquet, J., and Guieu, C.: Impact of dust addition on the metabolism of Mediterranean plankton communities and carbon export under present and future conditions of pH and temperature, Biogeosciences Discussions, 1–74, https://doi.org/10.5194/bg-2021-20, 2021.

Gorsky, G., Ohman, M. D., Picheral, M., Gasparini, S., Stemmann, L., Romagnan, J.-B., Cawood, A., Pesant, S., García-Comas, C., and Prejger, F.: Digital zooplankton image analysis using the ZooScan integrated system, J Plankton Res, 32, 285–303, https://doi.org/10.1093/plankt/fbp124, 2010.

Guieu, C. and Ridame, C.: Impact of atmospheric deposition on marine chemistry and biogeochemistry, in: Atmospheric Chemistry in the Mediterranean Region: Comprehensive Diagnosis and Impacts, edited by: Dulac, F., Sauvage, S., and Hamonou, E., Springer, Cham, Switzerland, 2020.

Guieu, C., Dulac, F., Desboeufs, K., Wagener, T., Pulido-Villena, E., Grisoni, J.-M., Louis, F., Ridame, C., Blain, S., Brunet, C., Bon Nguyen, E., Tran, S., Labiadh, M., and Dominici, J.-M.: Large clean mesocosms and simulated dust deposition: a new methodology to investigate responses of marine oligotrophic ecosystems to atmospheric inputs, 7, 2765–2784, https://doi.org/10.5194/bg-7-2765-2010, 2010a.

Guieu, C., Loye-Pilot, M. D., Benyahya, L., and Dufour, A.: Spatial variability of atmospheric fluxes of metals (Al, Fe, Cd, Zn and Pb) and phosphorus over the whole Mediterranean from a one-year monitoring experiment: Biogeochemical implications, 120, 164–178, https://doi.org/10.1016/j.marchem.2009.02.004, 2010b.

Guieu, C., Ridame, C., Pulido-Villena, E., Bressac, M., Desboeufs, K., and Dulac, F.: Impact of dust deposition on carbon budget: a tentative assessment from a mesocosm approach, 11, 5621–5635, 2014a.

Formatted: English (UK)

Deleted: Gazeau, F., Van Wambeke, F., Marañón, E., Pérez-Lorenzo, M., Alliouane, S., Stolpe, C., Blasco, T., Leblond, N., Zäncker, B., Engel, A., Marie, B., Dinasquet, J., and Guieu, C.: Impact of dust addition on the metabolism of Mediterranean plankton communities and carbon export under present and future conditions of pH and temperature, 2021.¶

Guieu, C., Aumont, O., Paytan, A., Bopp, L., Law, C. S., Mahowald, N., Achterberg, E. P., Marañón, E., Salihoglu, B., Crise, A., Wagener, T., Herut, B., Desboeufs, K., Kanakidou, M., Olgun, N., Peters, F., Pulido-Villena, E., Tovar-Sanchez, A., and Völker, C.: The significance of the episodic nature of atmospheric deposition to Low Nutrient Low Chlorophyll regions, 28, 1179–1198, https://doi.org/10.1002/2014GB004852, 2014b.

Guieu, C., D'Ortenzio, F., Dulac, F., Taillandier, V., Doglioli, A., Petrenko, A., Barrillon, S., Mallet, M., Nabat, P., and Desboeufs, K.: Process studies at the air-sea interface after atmospheric deposition in the Mediterranean Sea: objectives and strategy of the PEACETIME oceanographic campaign (May–June 2017), 2020, 5563–5585, https://doi.org/10.5194/bg-17-5563-2020, 2020.

Herut, B., Zohary, T., Krom, M. D., Mantoura, R. F. C., Pitta, P., Psarra, S., Rassoulzadegan, F., Tanaka, T., and Frede Thingstad, T.: Response of East Mediterranean surface water to Saharan dust: On-board microcosm experiment and field observations, Deep Sea Research Part II: Topical Studies in Oceanography, 52, 3024–3040, https://doi.org/10.1016/j.dsr2.2005.09.003, 2005.

Holmes, R. M., Aminot, A., Kérouel, R., Hooker, B. A., and Peterson, B. J.: A simple and precise method for measuring ammonium in marine and freshwater ecosystems, Can. J. Fish. Aquat. Sci., 56, 1801–1808, https://doi.org/10.1139/f99-128, 1999.

IPCC: Climate Change, The Physical Science Basis, 2013.

IPCC: IPCC Special Report on the Ocean and Cryosphere in a Changing Climate, edited by: Pörtner, H. O., Roberts, D. C., Masson-Delmotte, V., Zhai, P., Tignor, M., Poloczanska, E., Mintenbeck, K., Alegría, A., Nicolai, M., Okem, A., Petzold, J., Rama, B., and Weyer, N. M., 2019.

Irwin, A. J. and Oliver, M. J.: Are ocean deserts getting larger?, 36, https://doi.org/10.1029/2009gl039883, 2009.

Jickells, T. D., An, Z. S., Andersen, K. K., Baker, A. R., Bergametti, G., Brooks, N., Cao, J. J., Boyd, P. W., Duce, R. A., Hunter, K. A., Kawahata, H., Kubilay, N., laRoche, J., Liss, P. S., Mahowald, N., Prospero, J. M., Ridgwell, A. J., Tegen, I., and Torres, R.: Global Iron Connections Between Desert Dust, Ocean Biogeochemistry, and Climate, 308, 67–71, https://doi.org/10.1126/science.1105959, 2005.

Kana, T. M. and Glibert, P. M.: Effect of irradiances up to 2000 μE m^{-2} s^{-1} on marine *Synechococcus* WH7803—I. Growth, pigmentation, and cell composition, Deep Sea Research Part A. Oceanographic Research Papers, 34, 479–495, https://doi.org/10.1016/0198-0149(87)90001-X, 1987.

Kapsenberg, L., Alliouane, S., Gazeau, F., Mousseau, L., and Gattuso, J.-P.: Coastal ocean acidification and increasing total alkalinity in the northwestern Mediterranean Sea, 13, 411–426, https://doi.org/10.5194/os-13-411-2017, 2017.

Kouvarakis, G., Mihalopoulos, N., Tselepides, A., and Stavrakakis, S.: On the importance of atmospheric inputs of inorganic nitrogen species on the productivity of the Eastern Mediterranean Sea, 15, 805–817, https://doi.org/10.1029/2001GB001399, 2001.

Lagaria, A., Mandalakis, M., Mara, P., Papageorgiou, N., Pitta, P., Tsiola, A., Kagiorgi, M., and Psarra, S.: Phytoplankton response to Saharan dust depositions in the Eastern Mediterranean Sea: A mesocosm study, Front. Mar. Sci., 3, https://doi.org/10.3389/fmars.2016.00287, 2017.

Law, C. S., Brévière, E., de Leeuw, G., Garçon, V., Guieu, C., Kieber, D. J., Kontradowitz, S., Paulmier, A., Quinn, P. K., Saltzman, E. S., Stefels, J., and von Glasow, R.: Evolving research directions in Surface Ocean - Lower Atmosphere (SOLAS) science, Environ. Chem., 10, 1, https://doi.org/10.1071/EN12159, 2013.

Lee, S. and Fuhrman, J. A.: Relationships between Biovolume and Biomass of Naturally Derived Marine Bacterioplankton, Appl Environ Microbiol, 53, 1298–1303, 1987.

Lekunberri, I., Lefort, T., Romero, E., Vázquez-Domínguez, E., Romera-Castillo, C., Marrasé, C., Peters, F., Weinbauer, M., and Gasol, J. M.: Effects of a dust deposition event on coastal marine microbial abundance and activity, bacterial community structure and ecosystem function, J Plankton Res, 32, 381–396, https://doi.org/10.1093/plankt/fbp137, 2010.

Liu, X., Patsavas, M. C., and Byrne, R. H.: Purification and Characterization of meta-Cresol Purple for Spectrophotometric Seawater pH Measurements, Environ. Sci. Technol., 45, 4862–4868, https://doi.org/10.1021/es200665d, 2011.

Longhurst, A., Sathyendranath, S., Platt, T., and Caverhill, C.: An estimate of global primary production in the ocean from satellite radiometer data, 17, 1245–1271, https://doi.org/10.1093/plankt/17.6.1245, 1995.

López-Urrutia, A. and Morán, X. A. G.: Resource limitation of bacterial production distorts the temperature dependence of oceanic carbon cycling, Ecology, 88, 817–822, https://doi.org/10.1890/06-1641, 2007.

Louis, J., Pedrotti, M. L., Gazeau, F., and Guieu, C.: Experimental evidence of formation of transparent exopolymer particles (TEP) and POC export provoked by dust addition under current and high pCO_2 conditions, PLOS ONE, 12, e0171980, https://doi.org/10.1371/journal.pone.0171980, 2017a.

Louis, J., Guieu, C., and Gazeau, F.: Nutrient dynamics under different ocean acidification scenarios in a low nutrient low chlorophyll system: The Northwestern Mediterranean Sea, Estuarine, Coastal and Shelf Science, 186, 30–44, https://doi.org/10.1016/j.ecss.2016.01.015, 2017b.

Louis, J., Gazeau, F., and Guieu, C.: Atmospheric nutrients in seawater under current and high pCO_2 conditions after Saharan dust deposition: Results from three minicosm experiments, Progress in Oceanography, 163, 40–49, https://doi.org/10.1016/j.pocean.2017.10.011, 2018.

Loÿe-Pilot, M. D. and Martin, J. M.: Saharan Dust Input to the Western Mediterranean: An Eleven Years Record in Corsica, in: The Impact of Desert Dust Across the Mediterranean, edited by: Guerzoni, S. and Chester, R., Springer Netherlands, Dordrecht, 191–199, https://doi.org/10.1007/978-94-017-3354-0_18, 1996.

Manca, B., Burca, M., Giorgetti, A., Coatanoan, C., Garcia, M.-J., and Iona, A.: Physical and biochemical averaged vertical profiles in the Mediterranean regions: an important tool to trace the climatology of water masses and to validate incoming data from operational oceanography, Journal of Marine Systems, 48, 83–116, https://doi.org/10.1016/j.jmarsys.2003.11.025, 2004.

Marañón, E., Fernández, A., Mouriño-Carballido, B., MartÍnez-GarcÍa, S., Teira, E., Cermeño, P., Chouciño, P., Huete-Ortega, M., Fernández, E., Calvo-DÍaz, A., Morán, X. A. G., Bode, A., Moreno-Ostos, E., Varela, M. M., Patey, M. D., and Achterberg, E. P.: Degree of oligotrophy controls the response of microbial plankton to Saharan dust, 55, 2339–2352, https://doi.org/10.4319/lo.2010.55.6.2339, 2010.

Marañón, E., Lorenzo, M. P., Cermeño, P., and Mouriño-Carballido, B.: Nutrient limitation suppresses the temperature dependence of phytoplankton metabolic rates, 12, 1836–1845, https://doi.org/10.1038/s41396-018-0105-1, 2018.

Marie, D., Simon, N., Guillou, L., Partensky, F., and Vaulot, D.: Flow cytometry analysis of marine picoplankton, in: living color: protocols in flow cytometry and cell sorting, edited by: Diamond, R. A. and DeMaggio, S., Springer, Berlin, 421–454, 2010.

Markaki, Z., Oikonomou, K., Kocak, M., Kouvarakis, G., Chaniotaki, A., Kubilay, N., and Mihalopoulos, N.: Atmospheric deposition of inorganic phosphorus in the Levantine Basin, eastern Mediterranean: Spatial and temporal variability and its role in seawater productivity, 48, 1557–1568, https://doi.org/10.4319/lo.2003.48.4.1557, 2003.

Maugendre, L., Gattuso, J.-P., Louis, J., de Kluijver, A., Marro, S., Soetaert, K., and Gazeau, F.: Effect of ocean warming and acidification on a plankton community in the NW Mediterranean Sea, 72, 1744–1755, https://doi.org/10.1093/icesjms/fsu161, 2015.

Maugendre, L., Guieu, C., Gattuso, J.-P., and Gazeau, F.: Ocean acidification in the Mediterranean Sea: Pelagic mesocosm experiments. A synthesis, Estuarine, Coastal and Shelf Science, 186, 1–10, https://doi.org/10.1016/j.ecss.2017.01.006, 2017.

Mayot, N., D'Ortenzio, F., Ribera d'Alcalà, M., Lavigne, H., and Claustre, H.: Interannual variability of the Mediterranean trophic regimes from ocean color satellites, 13, 1901–1917, https://doi.org/10.5194/bg-13-1901-2016, 2016.

Mélançon, J., Levasseur, M., Lizotte, M., Scarratt, M., Tremblay, J.-É., Tortell, P., Yang, G.-P., Shi, G.-Y., Gao, H., Semeniuk, D., Robert, M., Arychuk, M., Johnson, K., Sutherland, N., Davelaar, M., Nemcek, N., Peña, A., and Richardson, W.: Impact of ocean acidification on phytoplankton assemblage, growth, and DMS production following Fe-dust additions in the NE Pacific high-nutrient, low-chlorophyll waters, 13, 1677–1692, https://doi.org/10.5194/bg-13-1677-2016, 2016.

Moore, C. M., Mills, M. M., Arrigo, K. R., Berman-Frank, I., Bopp, L., Boyd, P. W., Galbraith, E. D., Geider, R. J., Guieu, C., Jaccard, S. L., Jickells, T. D., La Roche, J., Lenton, T. M., Mahowald, N. M., Marañón, E., Marinov, I., Moore, J. K., Nakatsuka, T., Oschlies, A., Saito, M. A., Thingstad, T. F., Tsuda, A., and Ulloa, O.: Processes and patterns of oceanic nutrient limitation, 6, 701–710, https://doi.org/10.1038/ngeo1765, 2013.

Morán, X. A. G., López-Urrutia, Á., Calvo-Díaz, A., and Li, W. K. W.: Increasing importance of small phytoplankton in a warmer ocean, 16, 1137–1144, https://doi.org/10.1111/j.1365-2486.2009.01960.x, 2010.

Neale, P. J., Sobrino, C., Segovia, M., Mercado, J. M., Leon, P., Cortés, M. D., Tuite, P., Picazo, A., Salles, S., Cabrerizo, M. J., Prasil, O., Montecino, V., Reul, A., and Fuentes-Lema, A.:

1817 Effect of CO2, nutrients and light on coastal plankton. I. Abiotic conditions and biological
1818 responses, 22, 25–41, https://doi.org/10.3354/ab00587, 2014.
1819 Obernosterer, I., Kawasaki, N., and Benner, R.: P-limitation of respiration in the Sargasso Sea
1820 and uncoupling of bacteria from P-regeneration in size-fractionation experiments, 32, 229–
1821 237, https://doi.org/10.3354/ame032229, 2003.
1822 Orr, J. C., Epitalon, J.-M., Dickson, A. G., and Gattuso, J.-P.: Routine uncertainty propagation
1823 for the marine carbon dioxide system, 207, 84–107,
1824 https://doi.org/10.1016/j.marchem.2018.10.006, 2018.
1825 Paytan, A., Mackey, K. R. M., Chen, Y., Lima, I. D., Doney, S. C., Mahowald, N., Labiosa, R.,
1826 and Post, A. F.: Toxicity of atmospheric aerosols on marine phytoplankton, 106, 4601–
1827 4605, https://doi.org/10.1073/pnas.0811486106, 2009.
1828 Pitta, P., Kanakidou, M., Mihalopoulos, N., Christodoulaki, S., Dimitriou, P. D., Frangoulis, C.,
1829 Giannakourou, A., Kagiorgi, M., Lagaria, A., Nikolaou, P., Papageorgiou, N., Psarra, S.,
1830 Santi, I., Tsapakis, M., Tsiola, A., Violaki, K., and Petihakis, G.: Saharan Dust Deposition
1831 Effects on the Microbial Food Web in the Eastern Mediterranean: A Study Based on a
1832 Mesocosm Experiment, Front. Mar. Sci., 4, https://doi.org/10.3389/fmars.2017.00117,
1833 2017.
1834 Polovina, J. J., Howell, E. A., and Abecassis, M.: Ocean's least productive waters are expanding,
1835 35, https://doi.org/10.1029/2007gl031745, 2008.
1836 Powley, H. R., Krom, M. D., and Cappellen, P. V.: Understanding the unique biogeochemistry of
1837 the Mediterranean Sea: Insights from a coupled phosphorus and nitrogen model, 31, 1010–
1838 1031, https://doi.org/10.1002/2017GB005648, 2017.
1839 Pulido-Villena, E., Wagener, T., and Guieu, C.: Bacterial response to dust pulses in the western
1840 Mediterranean: Implications for carbon cycling in the oligotrophic ocean, 22,
1841 https://doi.org/10.1029/2007gb003091, 2008.

Pulido-Villena, E., Rerolle, V., and Guieu, C.: Transient fertilizing effect of dust in P-deficient LNLC surface ocean, 37, https://doi.org/10.1029/2009gl041415, 2010.

Pulido-Villena, E., Baudoux, A.-C., Obernosterer, I., Landa, M., Caparros, J., Catala, P., Georges, C., Harmand, J., and Guieu, C.: Microbial food web dynamics in response to a Saharan dust event: results from a mesocosm study in the oligotrophic Mediterranean Sea, 11, 5607–5619, 2014.

Putaud, J.-P., Dingenen, R. V., Dell'Acqua, A., Raes, F., Matta, E., Decesari, S., Facchini, M. C., and Fuzzi, S.: Size-segregated aerosol mass closure and chemical composition in Monte Cimone (I) during MINATROC, 4, 889–902, https://doi.org/10.5194/acp-4-889-2004, 2004.

Ras, J., Claustre, H., and Uitz, J.: Spatial variability of phytoplankton pigment distributions in the Subtropical South Pacific Ocean: comparison between in situ and predicted data, 5, 353–369, https://doi.org/10.5194/bg-5-353-2008, 2008.

Regaudie-de-Gioux, A., Vaquer-Sunyer, R., and Duarte, C. M.: Patterns in planktonic metabolism in the Mediterranean Sea, 6, 3081–3089, https://doi.org/10.5194/bg-6-3081-2009, 2009.

Richon, C., Dutay, J.-C., Dulac, F., Wang, R., Balkanski, Y., Nabat, P., Aumont, O., Desboeufs, K., Laurent, B., Guieu, C., Raimbault, P., and Beuvier, J.: Modeling the impacts of atmospheric deposition of nitrogen and desert dust-derived phosphorus on nutrients and biological budgets of the Mediterranean Sea, Progress in Oceanography, 163, 21–39, https://doi.org/10.1016/j.pocean.2017.04.009, 2018.

Ridame, C. and Guieu, C.: Saharan input of phosphate to the oligotrophic water of the open western Mediterranean Sea, 47, 856–869, 2002.

Ridame, C., Guieu, C., and L'Helguen, S.: Strong stimulation of N 2 fixation in oligotrophic Mediterranean Sea: results from dust addition in large in situ mesocosms, 10, 7333–7346, 2013.

Ridame, C., Dekaezemacker, J., Guieu, C., Bonnet, S., L'Helguen, S., and Malien, F.: Contrasted Saharan dust events in LNLC environments: impact on nutrient dynamics and primary production, 11, 4783–4800, 2014.

Romero, E., Peters, F., Marrasé, C., Guadayol, Ò., Gasol, J. M., and Weinbauer, M. G.: Coastal Mediterranean plankton stimulation dynamics through a dust storm event: An experimental simulation, Estuarine, Coastal and Shelf Science, 93, 27–39, https://doi.org/10.1016/j.ecss.2011.03.019, 2011.

Roy-Barman, M., Foliot, L., Douville, E., Leblond, N., Gazeau, F., Bressac, M., Wagener, T., Ridame, C., Desboeufs, K., and Guieu, C.: Contrasted release of insoluble elements (Fe, Al, rare earth elements, Th, Pa) after dust deposition in seawater: a tank experiment approach, Biogeosciences, 18, 2663–2678, https://doi.org/10.5194/bg-18-2663-2021, 2021.

Sala, M. M., Aparicio, F. L., Balagué, V., Boras, J. A., Borrull, E., Cardelús, C., Cros, L., Gomes, A., López-Sanz, A., Malits, A., Martínez, R. A., Mestre, M., Movilla, J., Sarmento, H., Vázquez-Domínguez, E., Vaqué, D., Pinhassi, J., Calbet, A., Calvo, E., Gasol, J. M., Pelejero, C., and Marrasé, C.: Contrasting effects of ocean acidification on the microbial food web under different trophic conditions, 73, 670–679, https://doi.org/10.1093/icesjms/fsv130, 2016.

Sherr, E. B. and Sherr, B. F.: Bacterivory and herbivory: Key roles of phagotrophic protists in pelagic food webs, Microb Ecol, 28, 223–235, https://doi.org/10.1007/BF00166812, 1994.

Siokou-Frangou, I., Christaki, U., Mazzocchi, M. G., Montresor, M., Ribera d'Alcalá, M., Vaqué, D., and Zingone, A.: Plankton in the open Mediterranean Sea: a review, 7, 1543–1586, https://doi.org/10.5194/bg-7-1543-2010, 2010.

Tanaka, T., Thingstad, T. F., Christaki, U., Colombet, J., Cornet-Barthaux, V., Courties, C., Grattepanche, J.-D., Lagaria, A., Nedoma, J., Oriol, L., Psarra, S., Pujo-Pay, M., and Wambeke, F. V.: Lack of P-limitation of phytoplankton and heterotrophic prokaryotes in

Formatted: English (UK)

Deleted: ¶
Roy-Barman, M., Folio, L., Douville, E., Leblond, N., Gazeau, F., Bressac, M., Wagener, T., Ridame, C., Desboeufs, K., and Guieu, C.: Contrasted release of insoluble elements (Fe, Al, REE, Th, Pa) after dust deposition in seawater: a tank experiment approach, 1–27, https://doi.org/10.5194/bg-2020-247, 2020.¶

surface waters of three anticyclonic eddies in the stratified Mediterranean Sea, 8, 525–538, https://doi.org/10.5194/bg-8-525-2011, 2011.

Ternon, E., Guieu, C., Loÿe-Pilot, M.-D., Leblond, N., Bosc, E., Gasser, B., Miquel, J.-C., and Martín, J.: The impact of Saharan dust on the particulate export in the water column of the North Western Mediterranean Sea, 7, 809–826, https://doi.org/10.5194/bg-7-809-2010, 2010.

The Mermex group: Marine ecosystems' responses to climatic and anthropogenic forcings in the Mediterranean, 91, 97–166, https://doi.org/10.1016/j.pocean.2011.02.003, 2011.

Theodosi, C., Markaki, Z., Tselepides, A., and Mihalopoulos, N.: The significance of atmospheric inputs of soluble and particulate major and trace metals to the eastern Mediterranean seawater, Marine Chemistry, 120, 154–163, https://doi.org/10.1016/j.marchem.2010.02.003, 2010.

Van Wambeke, F., Goutx, M., Striby, L., Sempéré, R., and Vidussi, F.: Bacterial dynamics during the transition from spring bloom to oligotrophy in the northwestern Mediterranean Sea: relationships with particulate detritus and dissolved organic matter, 212, 89–105, 2001.

Van Wambeke, F., Taillandier, V., Deboeufs, K., Pulido-Villena, E., Dinasquet, J., Engel, A., Marañón, E., Ridame, C., and Guieu, C.: Influence of atmospheric deposition on biogeochemical cycles in an oligotrophic ocean system, 1–51, https://doi.org/10.5194/bg-2020-411, 2020a.

Van Wambeke, F., Pulido, E., Dinasquet, J., Djaoudi, K., Engel, A., Garel, M., Guasco, S., Nunige, S., Taillandier, V., Zäncker, B., and Tamburini, C.: Spatial patterns of biphasic ectoenzymatic kinetics related to biogeochemical properties in the Mediterranean Sea, 1–38, https://doi.org/10.5194/bg-2020-253, 2020b.

Verity, P. G., Robertson, C. Y., Tronzo, C. R., Andrews, M. G., Nelson, J. R., and Sieracki, M. E.: Relationships between cell volume and the carbon and nitrogen content of marine

photosynthetic nanoplankton, 37, 1434–1446, https://doi.org/10.4319/lo.1992.37.7.1434, 1992.

Vidussi, F., Claustre, H., Manca, B. B., Luchetta, A., and Marty, J.-C.: Phytoplankton pigment distribution in relation to upper thermocline circulation in the eastern Mediterranean Sea during winter, 106, 19939–19956, https://doi.org/10.1029/1999JC000308, 2001.

Table 1. List of parameters and processes investigated during the three experiments at stations TYR, ION and FAST. Corresponding manuscripts are indicated. pH_T: pH on the total scale, A_T: total alkalinity, ^{13}C-C_T: ^{13}C signature of dissolved inorganic carbon, NO_x: nitrate + nitrite, DIP: dissolved inorganic phosphorus, $Si(OH)_4$: silicate, DFe: dissolved iron, DAl: dissolved aluminium, Th-REE-Pa: Thorium (^{230}Th and ^{232}Th), Rare Earth elements and Protactinium (^{231}Pa), POC: particulate organic carbon, DOC: dissolved organic carbon, ^{13}C-DOC: ^{13}C signature of dissolved organic carbon, TEP: transparent exopolymer particles, NCP/CR: net community production and community respiration (oxygen based), ^{14}C-PP: primary production based on ^{14}C incorporation.

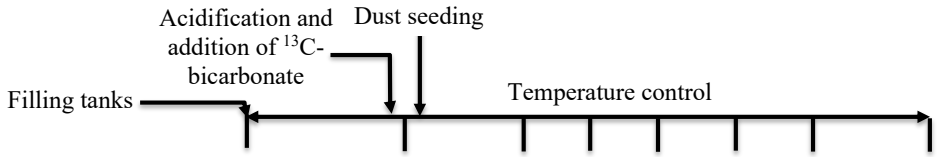

Sampling time	t-12h	t0	t1h	t6h	t12h	t24h	t48h	t72h / t96h	Related manuscript
	Hours post dust seeding								
Temperature	Continuous								This manuscript
Irradiance	Continuous								This manuscript

Carbonate chemistry

pH_T	This manuscript
A_T	This manuscript
$\delta^{13}C$-C_T	Gazeau et al. (2021)

Macro-nutrients

NO_x	This manuscript
DIP	This manuscript
$Si(OH)_4$	This manuscript

Micro-nutrients

DFe	Roy-Barman et al. (2021)
DAl	Roy-Barman et al. (2021)
Th-REE-Pa	Roy-Barman et al. (2021)

Biological stocks

Pigments	This manuscript
Flow cytometry	This manuscript

Deleted: 0

Deleted: 0

Deleted: 0

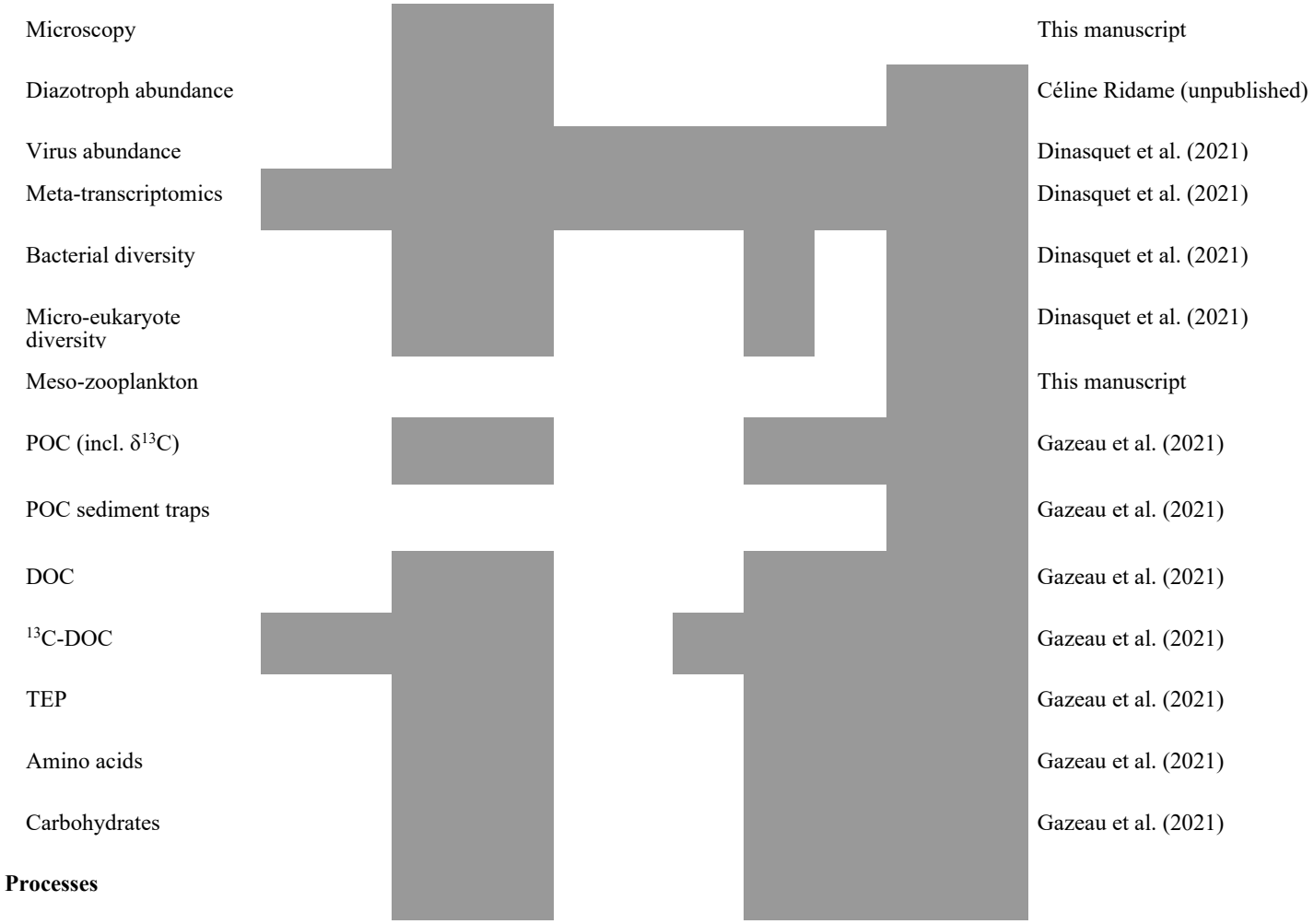
Microscopy
This manuscript
Diazotroph abundance
Céline Ridame (unpublished)
Virus abundance
Dinasquet et al. (2021)
Meta-transcriptomics
Dinasquet et al. (2021)
Bacterial diversity
Dinasquet et al. (2021)
Micro-eukaryote diversity
Dinasquet et al. (2021)
Meso-zooplankton
This manuscript
POC (incl. δ13C)
Gazeau et al. (2021)
POC sediment traps
Gazeau et al. (2021)
DOC
Gazeau et al. (2021)
13C-DOC
Gazeau et al. (2021)
TEP
Gazeau et al. (2021)
Amino acids
Gazeau et al. (2021)
Carbohydrates
Gazeau et al. (2021)
Processes

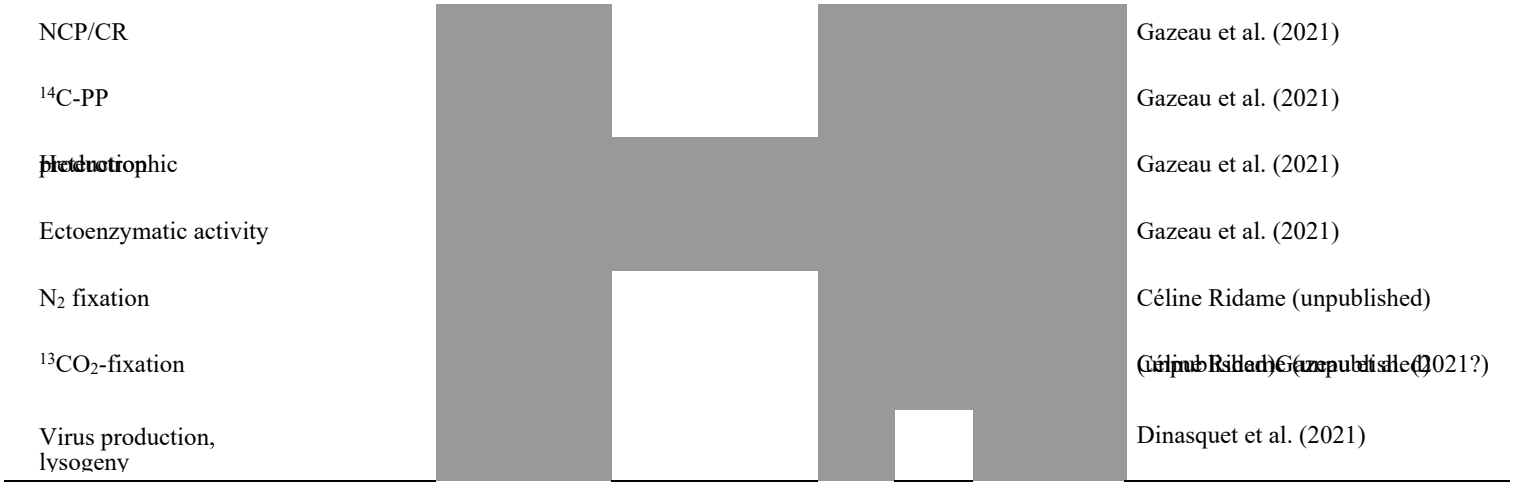
NCP/CR
Gazeau et al. (2021)
^{14}C-PP
Gazeau et al. (2021)
Heterotrophic prokaryotic production
Gazeau et al. (2021)
Ectoenzymatic activity
Gazeau et al. (2021)
N_2 fixation
Céline Ridame (unpublished)
$^{13}CO_2$-fixation
Céline Ridame (unpublished)
Virus production, lysogeny
Dinasquet et al. (2021)

1948

Table 2. Initial conditions (sampling time t-12h) at stations TYR, ION and FAST measured while filling the tanks. pH_T: pH on the total scale, NO_x: nitrate + nitrite, NH_4: ammonium, DIP: dissolved inorganic phosphorus, $Si(OH)_4$: silicate, TChl*a*: total chlorophyll *a*, HNF: heterotrophic nanoflagellates. The three most important pigments in terms of concentration are also presented (19'-hexanoyloxyfucoxanthin, Zeaxanthin and Divinyl Chlorophyll *a*). Biomasses of the different groups analyzed through flow cytometry were estimated based on conversion equations and/or factors found in the literature (see section 2.3). Autotrophic and heterotrophic biomass based on flow cytometry (fraction < 20 µm). Values below detection limits are indicated as < dl.

	Sampling station	TYR	ION	FAST
	Coordinates (decimal)	39.34 N, 12.60 E	35.49 N, 19.78 E	37.95 N, 2.90 N
	Bottom depth (m)	3395	3054	2775
	Day and time of sampling (local time)	17/05/2017 17:00	25/05/2017 17:00	02/06/2017 21:00
	Temperature (°C)	20.6	21.2	21.5
	Salinity	37.96	39.02	37.07
Carbonate chemistry	pH_T	8.04	8.07	8.03
	Total alkalinity (µmol kg^{-1})	2529	2627	2443
Nutrients	NO_x (nmol L^{-1})	14.0	18.0	59.0

Deleted: as

Deleted: (initial conditions in pumped surface water; sampling time: t-12h)

Deleted: was, as a first approximation, estimated only

Deleted: data and therefore corresponds to the

Deleted: Heterotrophic biomass was estimated as the sum of heterotrophic prokaryote and HNF biomasses (see section 2.3.2).…

	NH_4^+ (µmol L^{-1})	0.045	0.022	< dl
	DIP (nmol L^{-1})	17.1	6.5	12.9
	$Si(OH)_4$ (µmol L^{-1})	1.0	0.96	0.64
	NO_x/DIP (molar ratio)	0.8	2.5	4.6
Pigments	TChl*a* (µg L^{-1})	0.063	0.066	0.072
	19'-hexanoyloxyfucoxanthin (µg L^{-1})	0.017	0.021	0.016
	Zeaxanthin (µg L^{-1})	0.009	0.006	0.036
	Divinyl Chlorophyll *a* (µg L^{-1})	~ 0	0	0.014
Flow cytometry	Autotrophic pico-eukaryotes (cell mL^{-1}; biomass in µg C L^{-1})	347.8; 0.5	239.9; 0.4	701.0; 1.0
	Autotrophic nano-eukaryotes (cell mL^{-1}; biomass in µg C L^{-1})	150.5; 3.9	188.8; 4.8	196.6; 5.0
	Synechococcus (cell mL^{-1}; biomass in µg C L^{-1})	4972; 1.2	3037; 0.8	6406; 1.6
	Autotrophic biomass (µg C L^{-1})	5.6	6.0	7.7
	Heterotrophic prokaryotes abundance (x 10^5 cell mL^{-1})	4.79	2.14	6.15
	HNF (abundance in cell mL^{-1})	110.1	53.6	126.2
	Heterotrophic biomass (µg C L^{-1})	9.9	4.5	12.7
Microscopy	Pennate diatoms (abundance in cell L^{-1})	140	520	880
	Centric diatoms (abundance in cell L^{-1})	200	380	580
	Dinoflagellates (abundance in cell L^{-1})	2770	3000	3410
	Autotrophic flagellates (abundance in cell L^{-1})	0	60	650

Deleted: P

Deleted: abundance in

Deleted: N

Deleted: abundance in

Deleted: abundance in

Ciliates (abundance in cell L^{-1})	270	380	770

1971

Table 3. Maximum input of nitrate + nitrite (NO_x) and dissolved inorganic phosphorus (DIP) released from Saharan dust in tanks D and G as observed from the discrete samples taken during the first 6 h after seeding. The estimated maximal percentage of dissolution is also presented (see section 2.3.1 for details on the calculations).

	NO_x				DIP			
	D1	D2	G1	G2	D1	D2	G1	G2
Maximum input			$\mu mol\ L^{-1}$				$nmol\ L^{-1}$	
TYR	11.0	11.1	11.1	11.0	24.6	20.4	24.6	23.9
ION	11.2	11.6	11.2	11.3	23.3	22.0	19.6	22.9
FAST	11.3	11.1	11.1	11.2	30.8	31.3	36.9	29.8
Maximum dissolution (%)								
TYR	95	96	95	94	12	10	12	11
ION	96	99	96	97	11	10	9	11
FAST	97	97	95	97	15	15	17	14

Deleted: two
Deleted: ings
Deleted: performed
Deleted: over
Deleted: Percentage of

Table 4. Removal rate of nitrate + nitrite (NO_x) and dissolved inorganic phosphorus (DIP) in tanks D and G during the three experiments (TYR, ION and FAST). For NO_x, rates were estimated based on linear regressions between maximum concentrations (i.e. after dust enrichment, at t1h or t6h) and final concentrations (t72 h for TYR and ION and t96h for FAST). For DIP, rates were estimated based on linear regressions between maximum concentrations (i.e. after dust enrichment at t1h or t6h) and concentrations after stabilization was observed. This sampling time is shown in parentheses. All rates are expressed in nmol L^{-1} h^{-1}.

	NO_x			DIP		
	TYR	ION	FAST	TYR	ION	FAST
D1	-6.5	-8.6	-14.3	-0.4 (t72h)	-0.5 (t48h)	-0.2 (t96h)
D2	-1.0	-8.6	-13.5	-0.3 (t72h)	-0.8 (t24h)	-0.2 (t96h)
G1	-6.7	-13.1	-21.6	-1.3 (t24h)	-0.8 (t24h)	-1.5 (t24h)
G2	-0.8	-1.6	-25.2	-1.3 (t24h)	-1.6 (t24h)	-1.1 (t24h)

Deleted: decreasing

Deleted: al

Deleted: decreasing

Deleted: al

Deleted: measured at sampling times

Deleted: which a

Table 5. Percent (%) maximum relative changes in tanks D and G as compared to controls (average between C1 and C2), for the experiments TYR, ION and FAST. The sampling time at which these maximum relative changes were observed is shown in brackets. Tchl*a* refers to the concentration of total chlorophyll *a* and B_{micro} to the biomass proxy of micro-phytoplankton (sum of Fucoxanthin and Peridinin, see Material and Methods) based on high performance liquid chromatography (HPLC). HP and HNF refer to heterotrophic prokaryote and heterotrophic nanoflagellate abundances, respectively, measured by flow cytometry.

Experiment	Tank	HPLC		Flow cytometry				
		TChl*a*	B_{micro}	Autotrophic Pico-eukaryotes	Autotrophic Nano-eukaryotes	*Synechococcus*	HP	HNF
TYR	D1	-35 (t24h)	-33 (t12h)	-75 (t72h)	-80 (t1h)	-71 (t48h)	68 (t72h)	352 (t72h)
TYR	D2	-38 (t12h)	-39 (t24h)	-75 (t72h)	-80 (t1h)	-72 (t48h)	53 (t72h)	100 (t72h)
TYR	G1	60 (t72h)	52 (t72h)	-75 (t1h)	89 (t72h)	76 (t72h)	67 (t72h)	1095 (t72h)
TYR	G2	359 (t72h)	392 (t72h)	323 (t72h)	119 (t72h)	700 (t72h)	68 (t48h)	298 (t72h)
ION	D1	183 (t72h)	157 (t72h)	126 (t72h)	89 (t72h)	317 (t72h)	128 (t72h)	44 (t72h)

Deleted: M

Deleted: expressed as a %,

Deleted: three

Deleted: (

Deleted:)

Deleted: as

Formatted: Space Before: 0 pt, Line spacing: Double

Deleted: Nano-eukaryotes

ION	D2	109 (t72h)	156 (t72h)	117 (t72h)	-59 (t1h)	390 (t72h)	133 (t72h)	27 (t72h)
ION	G1	399 (t72h)	454 (t72h)	458 (t72h)	256 (t72h)	805 (t72h)	176 (t72h)	175 (t72h)
ION	G2	426 (t72h)	612 (t72h)	510 (t72h)	292 (t72h)	1425 (t72h)	161 (t72h)	129 (t72h)
FAST	D1	318 (t96h)	356 (t96h)	113 (t96h)	208 (t72h)	348 (t96h)	27 (t96h)	-38 (t96h)
FAST	D2	237 (t96h)	322 (t96h)	91 (t96h)	219 (t72h)	197 (t96h)	40 (t48h)	-49 (t96h)
FAST	G1	399 (t96h)	415 (t96h)	198 (t72h)	274 (t72h)	357 (t48h)	61 (t48h)	243 (t24h)
FAST	G2	395 (t96h)	421 (t96h)	129 (t72h)	202 (t96h)	344 (t48h)	67 (t48h)	74 (t24h)

Figure captions

Fig. 1. Location of the sampling stations in the Mediterranean Sea onboard the R/V "Pourquoi Pas ?" during the PEACETIME cruise. Background shows satellite-derived surface chlorophyll *a* concentration averaged over the entire duration of the cruise (Courtesy of Louise Rousselet).

Fig. 2. Diagram of an experimental tank (climate reactor).

Fig. 3. Proportion of the different pigments, as measured by high performance liquid chromatography (HPLC) in pumped surface seawater for the three experiments (t-12h).

Fig. 4. Continuous measurements of temperature and irradiance level (PAR) in the six tanks during the experiments at TYR, ION and FAST. The dashed vertical line indicates the time of dust seeding (after t0).

Fig. 5. pH on the total scale (pH_T) and total alkalinity (A_T) measured in the six tanks during the experiments at TYR, ION and FAST. The dashed vertical line indicates the time of dust seeding (after t0). Error bars correspond to the standard deviation based on analytical triplicates.

Fig. 6. Nutrients (nitrate + nitrite): NO_x, dissolved inorganic phosphorus: DIP, silicate: $Si(OH)_4$ and the molar ratio between NO_x and DIP, measured in each tank during the experiments at TYR, ION and FAST. The dashed vertical line indicates the time of seeding (after t0).

Fig. 7. Total chlorophyll *a* and major pigments, from high performance liquid chromatography (HPLC) measurements, in each tank during the experiments at TYR, ION and FAST. The dashed vertical line indicates the time of seeding (after t0).

Fig. 8. Abundance of autotrophic pico-eukaryotes, autotrophic nano-eukaryotes, *Synechococcus,* heterotrophic prokaryotes (HP), and heterotrophic nano-flagellates (HNF), measured by flow cytometry, in each tank during the experiments at TYR, ION and FAST. The evolution of

Deleted: ,
Deleted: on map of
Deleted: Scheme
Deleted: three
Deleted: three
Deleted: as well as
Deleted: the six
Deleted: s
Deleted: three
Deleted: Concentrations of t
Deleted: measured by
Deleted: the six
Deleted: s
Deleted: three
Deleted: in the six tanks during the three experiments.

autotrophic biomass (see Material and Methods for details on the calculation) is also shown. The dashed vertical line indicates the time of seeding (after t0).

Fig. 9. Abundances of meso-zooplankton species as measured in each tank at the end of the experiments at TYR, ION and FAST.

Fig. 10. Maximum relative change (%) of main biological stocks (TCHl*a*: total chlorophyll *a*, HP: heterotrophic prokaryotes) and processes (BP: bacterial production; PP: ^{14}C-based primary production; see Gazeau et al., 2021; BR: bacterial respiration (no data from this study); and N_2 fixation, Céline Ridame, unpublished results) obtained during the present study at the three stations (TYR, ION and FAST) under ambient conditions of pH and temperature (open red squares) and future conditions (full green squares). Vertical extension of each squares are delimited by the range of responses observed among the duplicates for each treatment. The dotted green squares for station TYR highlight the large variability observed between duplicates for some parameters and processes that prevented drawing solid conclusions. Box-plots (Med) represent the distribution of responses observed from studies conducted in the Mediterranean Sea, as compiled by Guieu and Ridame (2020).

Deleted: each experiment

Deleted: .

Deleted: al

Deleted: as

Deleted: 3

Deleted: S

Deleted: denote

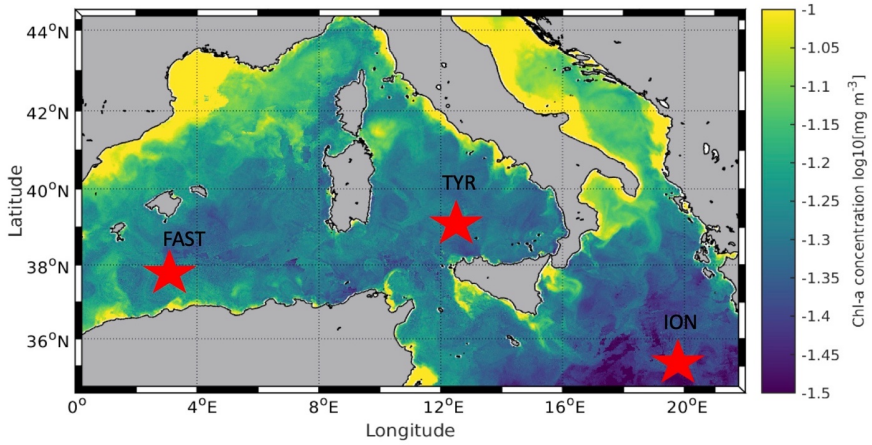
44°N
42°N
40°N
38°N
36°N
Latitude
0°
4°E
8°E
12°E
16°E
20°E
Longitude
FAST
TYR
ION
-1
-1.05
-1.1
-1.15
-1.2
-1.25
-1.3
-1.35
-1.4
-1.45
-1.5
Chl-a concentration log10[mg m-3]

Fig. 1.

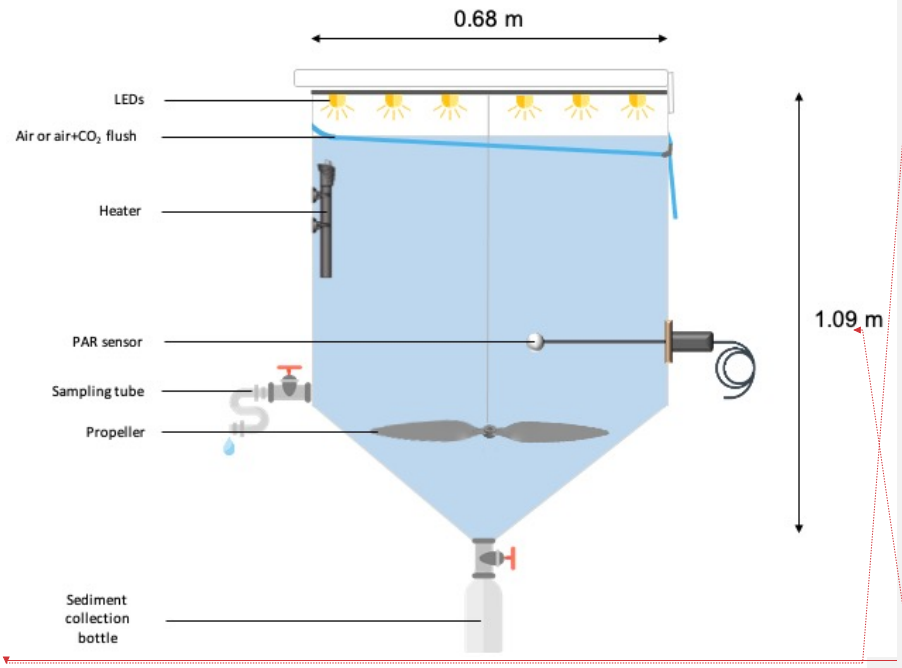

Deleted:

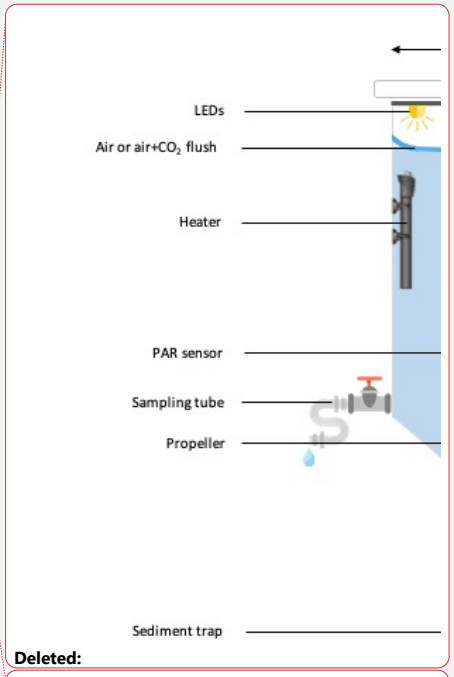

Formatted: Indent: First line: 1.27 cm

Fig. 2.

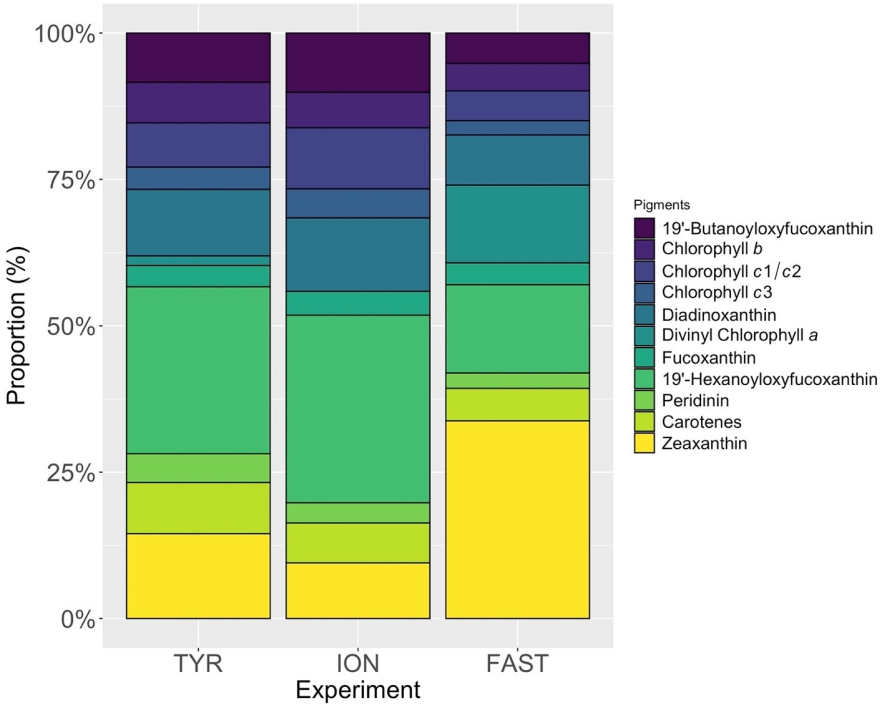
100%
75%
50%
25%
0%
Proportion (%)
TYR
ION
FAST
Experiment
Pigments
19'-Butanoyloxyfucoxanthin
Chlorophyll b
Chlorophyll c1/c2
Chlorophyll c3
Diadinoxanthin
Divinyl Chlorophyll a
Fucoxanthin
19'-Hexanoyloxyfucoxanthin
Peridinin
Carotenes
Zeaxanthin

Fig. 3.

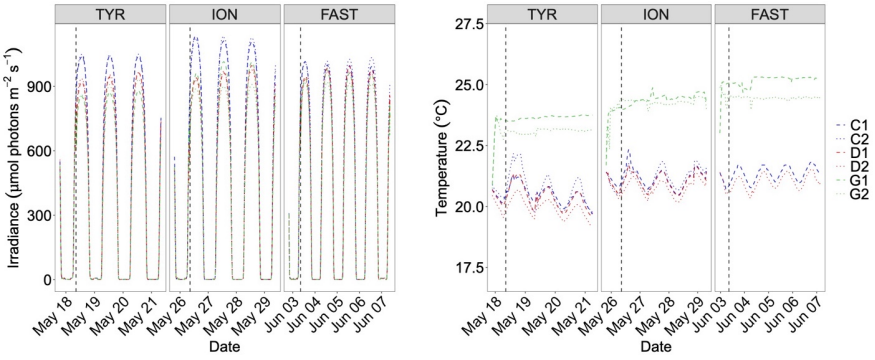
TYR
ION
FAST
Irradiance (µmol photons m^{-2} s^{-1})
0
300
600
900
Temperature (°C)
17.5
20.0
22.5
25.0
27.5
May 18
May 19
May 20
May 21
May 26
May 27
May 28
May 29
Jun 03
Jun 04
Jun 05
Jun 06
Jun 07
Date
C1
C2
D1
D2
G1
G2

Fig. 4.

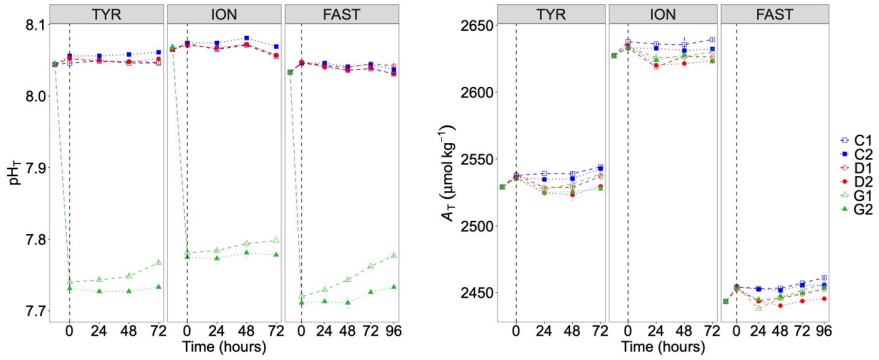
TYR
ION
FAST
8.1
8.0
7.9
7.8
7.7
pH$_T$
0 24 48 72
0 24 48 72
0 24 48 72 96
Time (hours)
TYR
ION
FAST
2650
2600
2550
2500
2450
A_T (µmol kg^{-1})
0 24 48 72
0 24 48 72
0 24 48 72 96
Time (hours)
C1
C2
D1
D2
G1
G2

Fig. 5.

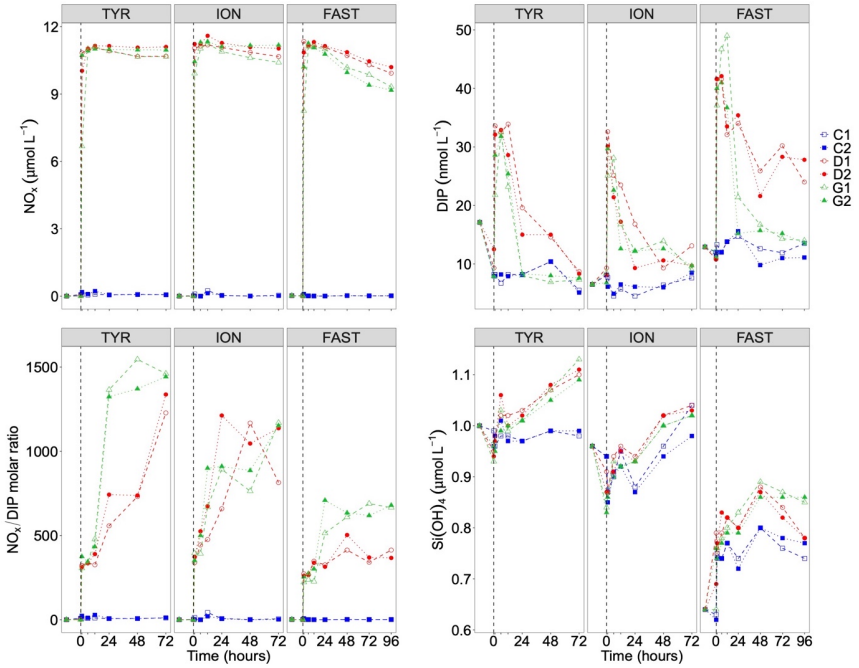
TYR
ION
FAST
NOx (µmol L−1)
DIP (nmol L−1)
NOx/DIP molar ratio
Si(OH)4 (µmol L−1)
Time (hours)
C1
C2
D1
D2
G1
G2

Fig. 6.

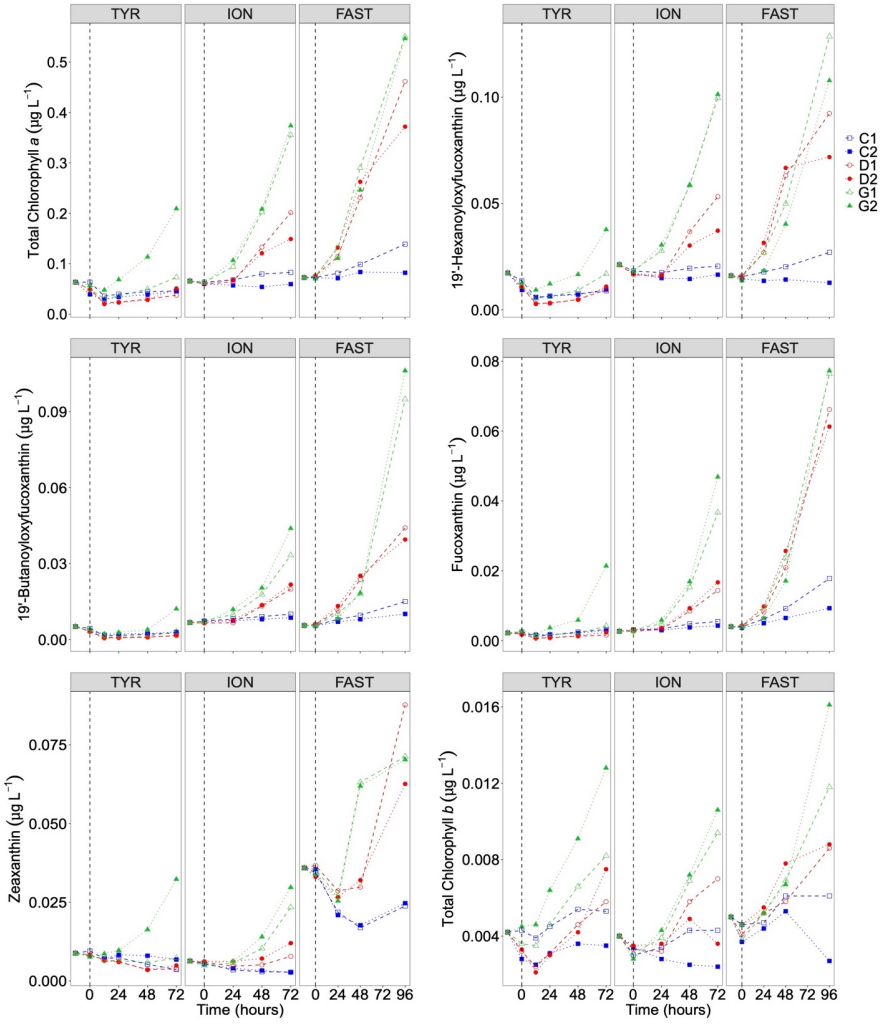
TYR
ION
FAST
Total Chlorophyll a (µg L⁻¹)
19'-Hexanoyloxyfucoxanthin (µg L⁻¹)
19'-Butanoyloxyfucoxanthin (µg L⁻¹)
Fucoxanthin (µg L⁻¹)
Zeaxanthin (µg L⁻¹)
Total Chlorophyll b (µg L⁻¹)
Time (hours)
C1
C2
D1
D2
G1
G2

Fig. 7.

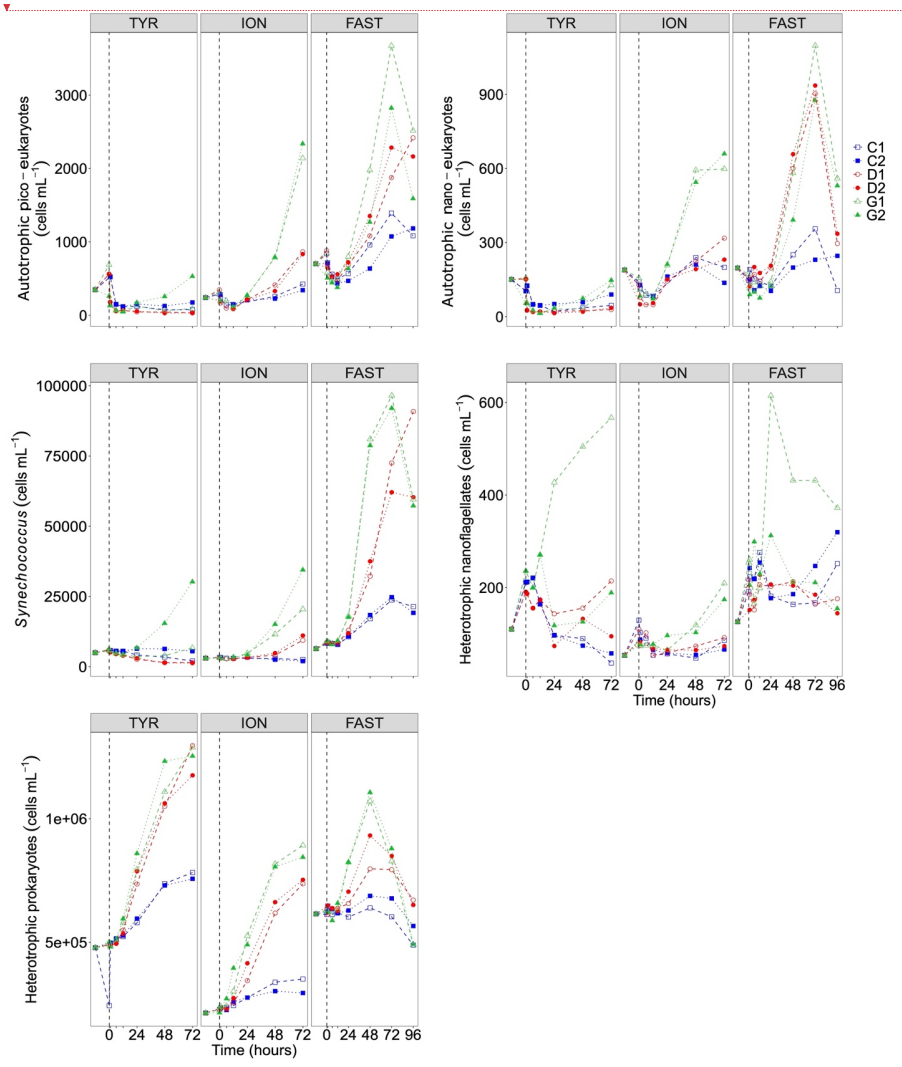

Deleted:

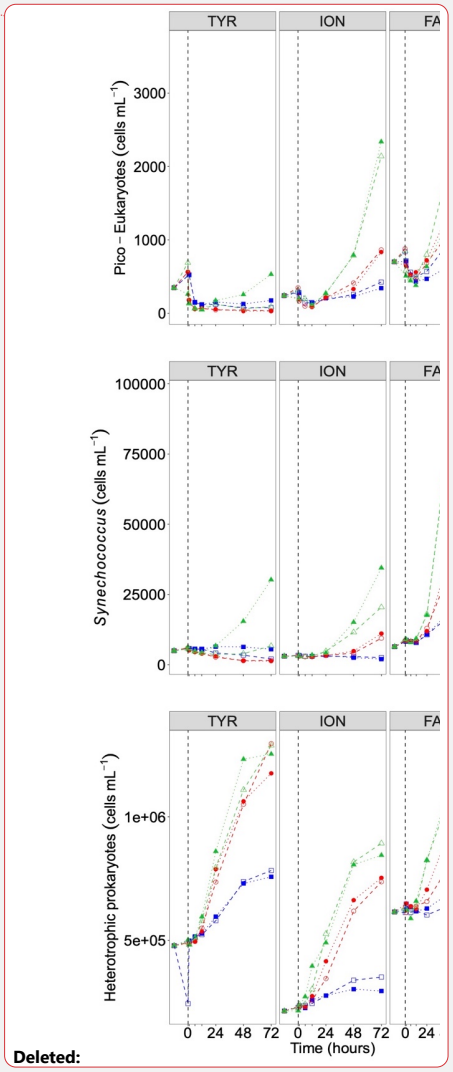

Fig. 8.

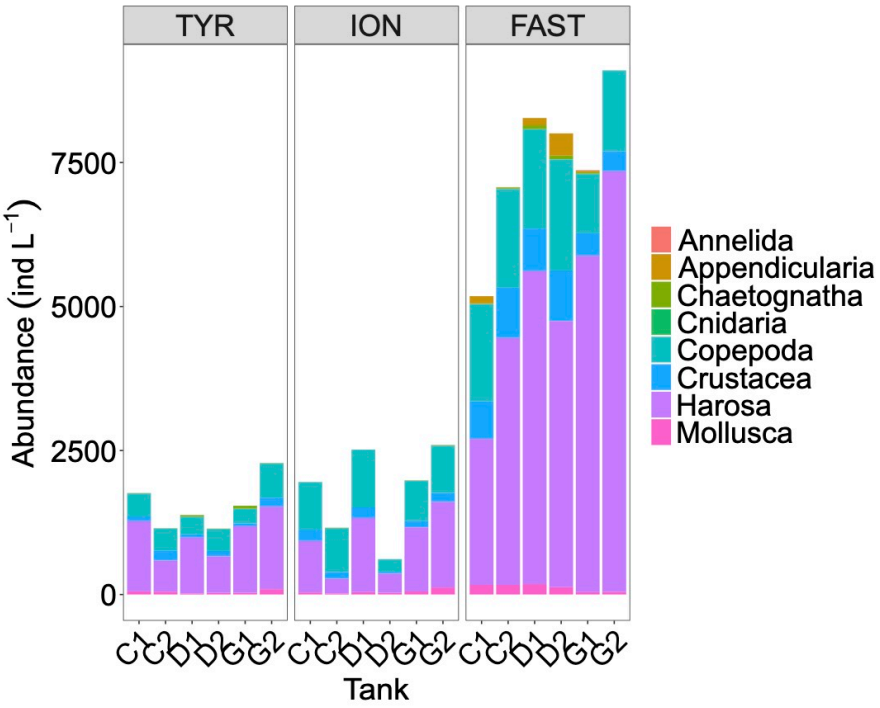
TYR
ION
FAST
7500
5000
2500
0
Abundance (ind L^{-1})
C1
C2
B1
B2
D1
D2
G1
G2
Tank
Annelida
Appendicularia
Chaetognatha
Cnidaria
Copepoda
Crustacea
Harosa
Mollusca

Fig. 9.

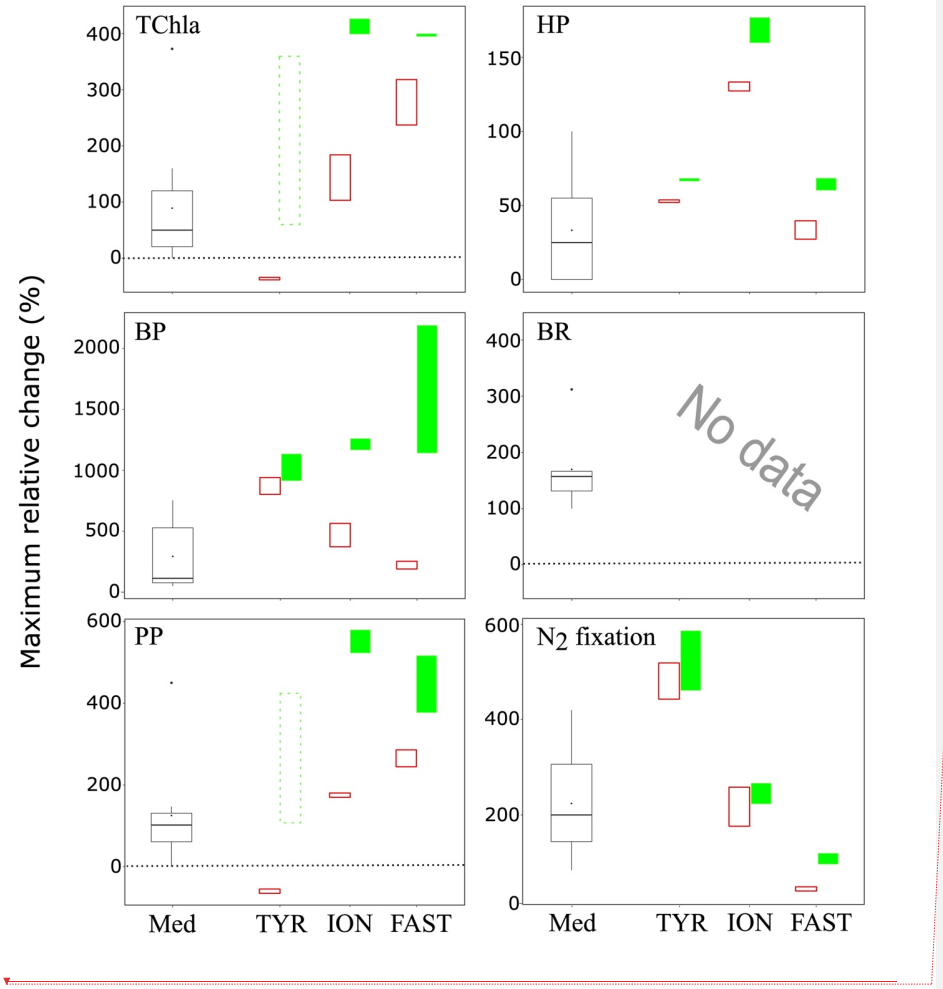

Deleted:

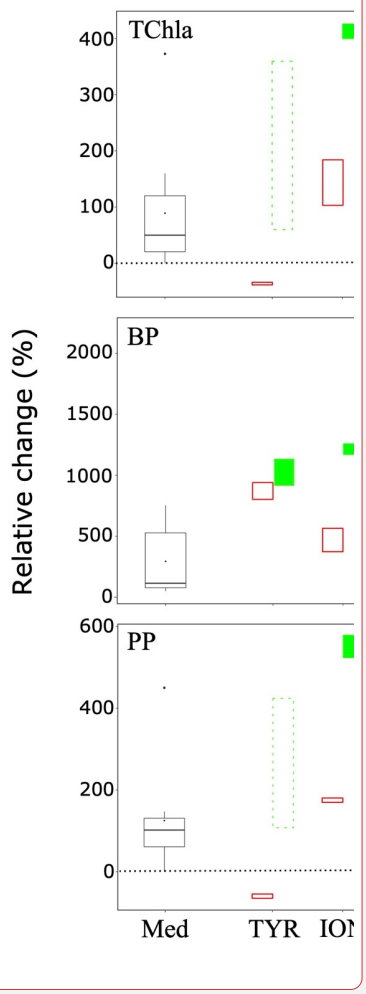

Fig. 10.

Page 14: [1] Deleted **Frederic GAZEAU** **13/06/2021 14:16:00**

Page 14: [2] Formatted **Frederic GAZEAU** **13/06/2021 14:14:00**

Formatted

Page 14: [3] Deleted **Frederic GAZEAU** **13/06/2021 14:20:00**

Page 14: [4] Deleted **Frederic GAZEAU** **13/06/2021 14:24:00**

Page 14: [5] Formatted **Frederic GAZEAU** **13/06/2021 14:25:00**

English (US)

Page 14: [6] Formatted **Frederic GAZEAU** **13/06/2021 14:28:00**

English (US)

Page 14: [7] Deleted **Frederic GAZEAU** **13/06/2021 14:32:00**